Hindawi
Contrast Media & Molecular Imaging
Volume 2018, Article ID 9713691, 24 pages
https://doi.org/10.1155/2018/9713691

Review Article

Prospective of ^{68}Ga Radionuclide Contribution to the Development of Imaging Agents for Infection and Inflammation

Irina Velikyan [1,2,3]

[1] *Section of Nuclear Medicine and PET, Department of Surgical Sciences, Uppsala University, Uppsala, Sweden*
[2] *Preclinical PET Platform, Department of Medicinal Chemistry, Uppsala University, Uppsala, Sweden*
[3] *PET Centre, Centre for Medical Imaging, Uppsala University Hospital, 75185 Uppsala, Sweden*

Correspondence should be addressed to Irina Velikyan; irina.velikyan@akademiska.se

Received 17 September 2017; Revised 19 November 2017; Accepted 10 December 2017; Published 4 January 2018

Academic Editor: Xiang-Guo Li

During the last decade, the utilization of ^{68}Ga for the development of imaging agents has increased considerably with the leading position in the oncology. The imaging of infection and inflammation is lagging despite strong unmet medical needs. This review presents the potential routes for the development of ^{68}Ga-based agents for the imaging and quantification of infection and inflammation in various diseases and connection of the diagnosis to the treatment for the individualized patient management.

1. Introduction

The blossom of ^{68}Ga utilization is reflected in the continuous rapid growth of the number of basic and clinical research publications as well as clinical trials and clinical practice [1–3]. The potential scope of ^{68}Ga-based imaging agents is rather extensive including ligands specifically targeting receptors, enzymes, and antigens; hapten and effector molecules involved in pretargeted imaging; small molecules with biological function to monitor glycolysis, hypoxia, cell proliferation, and angiogenesis; nontargeting particles of various sizes for imaging of ventilation and perfusion [4]. The leading clinical application area is oncology with targeted imaging of somatostatin receptors (SSTR), prostate specific membrane antigen (PSMA), integrin receptors, glucagon-like peptide 1 receptors (GLP1R), gastrin-releasing peptide receptors (GRPR), human epidermal growth factor receptor family (HER2), and pretargeted imaging of carcinoembryonic antigen (CEA) [1, 3, 5].

The scope of ^{68}Ga-based imaging agents for inflammation and infection is rather limited despite disease diversity and magnitude, and strong unmet medical need [1, 4, 6]. However, the research and development of ^{68}Ga-based tracers for the diagnosis and discrimination of inflammation and infection accelerated during last five years [7–19]. Such ^{68}Ga-based tracers with specific action could also considerably contribute to drug development. Unfortunately, the failure rate of new therapeutic drugs, in general, is rather high and it is a costly process. PET offers advantages such as possibility of quantifying the target occupancy by the drug very early in the development in vivo in humans due to the microdosing concept thus facilitating stratification of candidate therapeutic drugs.

This review presents the status of the ^{68}Ga-based imaging agents for inflammation and infection and discusses the potential routes for the development of the agents and their connection to the treatment for the individualized patient management.

2. Infection and Inflammation

Infection is caused by the invasion of such pathogens as bacteria, virus, fungi, parasite, or prion. It is a significant cause of morbidity and mortality globally, especially in children causing more death than any other disease. Tuberculosis, malaria, and AIDS stand for about 50% of all lethal cases claiming 5 million lives and causing 300 million illnesses each year. Bacterial infection, for example, tuberculosis and multidrug resistant bacteria, presents diagnostic and therapeutic challenges [20, 21]. Inflammation is immune response to microbial invasion or an injury and can either be

related to the pathogens or be sterile. It can be classified as acute or chronic, and the latter has been investigated as the major cause of inflammatory autoimmune, cardiovascular, neurological, and cancerous diseases.

In order to control infectious diseases and provide efficient treatment, early diagnosis as well as discrimination between bacterial and sterile inflammation is crucial. The disease specificity of the diagnostic tools is a desirable characteristic. Currently available diagnostic means present some disadvantages. Clinical laboratory tests such as white blood cell (WBC) counts and C-reactive protein (CRP) cannot unambiguously distinguish between bacterial and viral infection and may result in unnecessary treatment with antibiotics [22]. Radiological imaging techniques such as magnetic resonance imaging (MRI), X-ray, computed tomography (CT), and ultrasound are morphological and rely on the anatomical changes that occur at later stage of the disease. Moreover, these methods are not specific to neither inflammation nor infection type. Detection of viral infection is even more challenging since it does not produce anatomic changes as bacterial infection does even when the viral infection is severe.

In contrast to morphological imaging techniques, functional methods such as gamma scintigraphy (Single Photon Emission Computed Tomography (SPECT) and planar gamma imaging) and Positron Emission Tomography (PET) provide fast, whole-body, and noninvasive real time evaluation of physiology and pathology on molecular level early in disease processes before noticeable changes in anatomical structure occur. The whole-body examination might be of great importance especially in cases of occult infection [23]. The respective examinations can be repeated in order to monitor the treatment outcome resulting in personalized medicine approach [24–27]. The advantages of PET over SPECT are intrinsic to the technology and are presented with higher examination throughput, considerably higher sensitivity, possibility of detection, and quantification of tracer picomolar amounts as well as tracer uptake kinetics recording and dynamic image reconstruction [28]. In recent years, the stand-alone PET scanners have been substituted with hybrid PET-CT scanners that offer both high sensitivity of functional PET and temporal/spatial resolution of morphological CT in one examination. The hybrid PET-MRI scanners have also entered market providing advantages of MRI over CT in higher soft tissue contrast and absence of radiation dose to the patient. PET has demonstrated efficiency and profitability in individualized patient diagnostics especially in oncology, and its impact on patient management has been recognized by Medicare and Medicaid Services [29].

2.1. Common Clinical Imaging Agents for Inflammation and Infection. There are a few radiopharmaceuticals used in clinical routine, and they are nonspecific in their action: ^{67}Ga-Citrate, ^{99m}Tc/^{111}In-white blood cells (WBC), and [^{18}F]-fluorodeoxyglucose ([^{18}F]FDG) [30]. They target components of inflammatory response to injury and infection and accumulate in the lesions as a result of an increased blood flow and enhanced vascular permeability. ^{67}Ga-Citrate presumably transfers ^{67}Ga to transferrin and lactoferrin that accumulate at the inflammation site on the cells such as leukocytes and B-lymphocytes expressing respective receptors [31]. Moreover, ^{67}Ga can be accumulated in the macrophages, bacteria, and fungi via siderophores. Radiolabelled WBCs accumulate in the sites of leukocyte infiltration and do not discriminate infective from sterile inflammation [32]. [^{18}F]FDG accumulates in leukocytes, macrophages, monocytes, lymphocytes, and giant cells due to upregulation of glucose transporters [33].

^{67}Ga-Citrate has been in clinical use for imaging of infection and inflammation for over 40 years. It is applicable, for example, for the diagnosis of lung infections, acute/chronic osteomyelitis, tuberculosis, sarcoidosis, and retroperitoneal fibrosis [34]. However, the specificity of the agent is suboptimal with accumulation in malignancies and bone remodeling sites as well as bowel excretion pathway. Moreover, radiation doses to the healthy organs and tissues are unfavorable and the examination requires several visits to the hospital with an interval of 1–3 days between radiopharmaceutical administration and examination.

Radiolabelled autologous WBCs have been used for a wide range of infections such as peripheral osteomyelitis, postoperative infection, joint prosthesis infection, diabetic foot infection, cardiovascular infection, fever of unknown origin (FUO), opportunistic infection, central nervous system infection, musculoskeletal infection, and inflammatory bowel disease for over three decades. Various labelling techniques using ^{111}In-oxine, ^{99m}Tc-sulfur colloids, and ^{99m}Tc-exametazime (HMPAO) have been developed; however the radiopharmaceutical preparation procedure is complicated and potentially hazardous for both personnel and patient [21, 30]. Moreover, the examination process is very demanding on the patient [35].

Most nuclear medicine applications worldwide (90%) stand for diagnostics with leading position for ^{99m}Tc-based radiopharmaceuticals, especially in cardiology [36]. The most essential contribution to the improvement of the patient management in oncology has been presented by [^{18}F]-fluorodeoxyglucose ([^{18}F]FDG)/PET-CT reflecting the elevation of glucose transporter expression in tumour cells, and providing nearly universal application in the evaluation of various fast growing cancer types. [^{18}F]FDG/PET-CT stands for over 90% of all PET-CT examinations [37, 38]. [^{18}F]FDG/PET is an established diagnostic means also in infection and inflammation, and the major indications for it are FUO, sarcoidosis, peripheral bone osteomyelitis, suspected spinal infection, metastatic infection, bacteremia, and vasculitis [33]. However, demand for the imaging agents towards disease specific targets in cancer and inflammation/infection is growing [39, 40] since [^{18}F]FDG fails to detect slowly growing tumours and to discriminate malignancy from sterile inflammation, infection, wound healing, tuberculosis, sarcoidosis, and reactive lymph nodes [41, 42]. Another disadvantage is high accumulation of [^{18}F]FDG in healthy organs such as brain and gut resulting in suboptimal image contrast and consequently potential risk for lesion detection failure.

Table 1: Positron-emitting, gamma-emitting, and therapeutic radionuclides, their physical characteristics, and production mode. Adapted from [4].

Radionuclide	Half-life	E_{max} (keV)	Radiation	Production
		Positron emitters		
^{18}F	110 min	634	β^+ (97%)	Accelerator
^{64}Cu	12.8 h	656	β^+ (19%)	Accelerator
^{68}Ga	67.6 min	1899, 770	β^+ (89%)	Generator
^{89}Zr	78.4 h	900	β^+ (23%)	Accelerator
^{124}I	4.17 d	2100	β^+ (23%)	Accelerator
		Gamma emitters		
^{67}Ga	78.26 h	91, 93, 185, 296, 388	γ	Accelerator
^{99m}Tc	6.0 h	141	γ	Generator
^{111}In	67.9 h	245, 172 (0.5–25)	γ, Auger electrons	Accelerator
^{123}I	13.3 h	159	γ	Accelerator
		Therapeutic radionuclides		
^{177}Lu	6.71 d	113, 208.4 (598)	γ (β^-)	Reactor

2.2. Unmet Medical Need. Noninvasive and specific diagnosis of many inflammatory diseases such as sarcoidosis, osteomyelitis, inflammatory bowel disease, and rheumatoid arthritis as well as early and accurate diagnosis of deep-seated infectious diseases such as septic arthritis, abscesses, endocarditis, and infections of prosthetics and implants would benefit patients [20]. Introduction of specific imaging agents disclosing cellular mechanisms of various diseases on molecular level would allow improvement in patient management and treatment outcome. There is a strong need for specific imaging agents not only for the accurate and quantitative diagnosis but also for the prognosis, treatment selection, planning, and adjustment as well as response monitoring as, for example, requirement for a certain antibiotic and treatment duration. Moreover, the imaging could guide surgical procedures and monitor implants of medical devices or transplanted organs [43]. Such imaging guided treatment would decrease the cost, side effects, and overtreatment avoiding immune suppression effects in inflammation and possibly reducing the problem of antimicrobial resistance by the termination of an accomplished successful treatment as early as possible. There are potential challenges in targeting both components of inflammatory response and microbes specifically: discrimination between infectious and sterile inflammation; discrimination between acute and chronic inflammation; discrimination between various infectious microorganisms; discrimination between pathogenic bacteria and microbiota; targeting specific types of bacteria; difficulty of accessing bacteria aggregated in a biofilm; and quantification of reproducing bacteria.

Health care requires further improvement of efficiency, safety, and quality of treatment with patient personalized approach that would allow early diagnosis which is a crucial factor in the reduction of mortality and patient management cost [81]. The concept of individualized patient management on molecular level with regard to both diagnostics and therapy is based on discoveries and success in genomics, proteomics, and biotechnology. Those achievements also accelerate the development of various imaging agents, and the application of molecular imaging diagnostic techniques is expanding very fast globally contributing considerably to the realization of personalized medicine.

3. Advantages of ^{68}Ga: Nuclide Properties and Chemistry

Such radionuclides as ^{11}C, ^{18}F, ^{64}Cu, ^{68}Ga, ^{89}Zr, ^{99m}Tc, ^{111}In, and ^{124}I are used in various radiopharmaceuticals for diagnostic imaging with PET and SPECT (Table 1). With regard to PET, ^{18}F stands for 41%, ^{11}C stands for 31%, and ^{64}Cu, ^{68}Ga, ^{89}Zr, and ^{124}I stand for 28% of the radiopharmaceuticals [82]. With regard to SPECT, ^{99m}Tc and ^{111}In stand, respectively, for 42% and 29% of the radiopharmaceuticals. As mentioned above in the field of inflammation and infection gamma emitting ^{67}Ga, ^{99m}Tc, ^{111}In, and positron-emitting ^{18}F are commonly in use. The choice of a radionuclide depends on various aspects of production and application: availability, production mode, and cost of the radionuclide; nuclear characteristics and decay mode of the radionuclide; labelling chemistry pathways and duration; radiation dose to subjects; relevance of the physical half-life of the radionuclide to the pharmacokinetic time frame of the imaging agent. Within the group of gamma emitters used for SPECT, the production via generator system is an advantage that contributes to the leading position of ^{99m}Tc due to ready accessibility and lower cost. Moreover, the single and lower gamma energy of ^{99m}Tc results in higher image resolution as compared to ^{67}Ga and ^{111}In and shorter half-life of ^{99m}Tc reduces radiation dose to the patient (Table 2).

The advantages of PET such as higher spatial resolution, sensitivity, and accurate signal quantification are crucial, especially in the case of small size lesions. Furthermore, dynamic scanning allows modeling and investigation of the mechanism of the interaction between the imaging agent and target. Even though ^{68}Ga has a relatively high positron energy, the resolution of the images is comparable to that of ^{18}F, since it is the scanner detector resolution (4–6 mm)

Table 2: Effective doses for some PET and SPECT imaging agents. Reproduced from [6].

Agent	Examination time	Effective dose, [mSv]
[^{111}In]In-DTPA-octreotide/SPECT	24–48 h	10.8
[^{68}Ga]Ga-DOTA-TOC/PET	30–60 min	2.3
[^{18}F]FDG/PET	60–120 min	5.6
[^{99m}Tc]-BPAMD/SPECT	2–6 h	6
[^{99m}Tc]-MDP/SPECT	2–6 h	3-4
[^{68}Ga]Ga-BPAMD/PET	30–60 min	3-4

which is the limiting factor [4, 83, 84]. The 68-min half-life of ^{68}Ga is not compatible with ligands of slow pharmacokinetics, for example, antibodies. Thus other positron emitters such as ^{124}I, ^{89}Zr, and ^{64}Cu with longer half-lives allowing 2–4 days required for the clearance of the agent for the blood circulation and washout for the nontarget tissue are more relevant. The relatively short half-life of ^{68}Ga presents advantage in cases when repetitive examinations on the same day are of interest [85]. The high fraction of positron emission is another advantage of ^{68}Ga (89%) as compared to ^{64}Cu (19%) and ^{124}I (23%). Comparison of some clinically used imaging agents demonstrates the lower effective dose that patient is exposed to when using ^{68}Ga-based agent as compared to the agents comprising ^{18}F, ^{99m}Tc, and ^{111}In (Table 2) [6, 86, 87]. Moreover, the duration of patient examinations is shorter for ^{68}Ga-agents than that for SPECT agents, and to some extend for [^{18}F]FDG. In summary, the use of ^{68}Ga would be beneficial in terms of accessibility, high sensitivity and resolution, quantification, dynamic scanning, fast scanning protocol, repetitive examinations, and low radiation burden.

The chemical form in aqueous solution is Ga(III) cation which provides robust coordination chemistry. ^{68}Ga-labelling can be direct or chelator mediated. The direct labelling utilizes the chelating ability of macromolecules, for example, lactoferrin and transferrin comprising Tyr, His, and Asp AA residues that can chelate Ga(III) in the presence of synergetic bicarbonate ion. Low molecular weight ligands can form stable complexes of variable lipophilicity and charge for nontargeting imaging. The chelator mediated ^{68}Ga-labelling requires presence of a bifunctional chelator (BFC) for the subsequent, straightforward, and side specific coordination with Ga(III). Considerable number of chelators was successfully developed [4, 6, 88–95]. The most commonly used are DOTA and NOTA based chelators. The former requires heating under over 60°C for the complexation with ^{68}Ga, while the latter can chelate ^{68}Ga at ambient temperature which might be crucial in case of temperature sensitive ligands, and it also allows for cold kit type radiopharmaceutical preparation under radiopharmacy practice [96]. DOTA presents an advantage in the context of radiotheranostics since it can form stable complexes with ^{68}Ga for PET diagnostics and ^{177}Lu for radiotherapy.

The chelator or prosthetic group mediated labelling most commonly results in agents comprising biologically active vector molecule, chelator/prosthetic group moiety, and radionuclide. Very often pharmacokinetic modifiers (PKM) are incorporated in order to modulate pharmacokinetics and agent organ distribution and improve in vivo stability as well as separate the binding site from the bulky chelator/prosthetic group moiety which may deteriorate the biological activity of the vector molecule. Considerable number of publications reveal strong influence of even slight modifications in any of the agent structural components, and the accurate prediction of pharmacokinetics and pharmacodynamics of a new agent is not straightforward [97]. Nevertheless, vast experience and knowledge have been intensively gathered during last two decades providing possibility for more efficient and effective development. The labelling chemistry of ^{68}Ga is well characterized and is relevant to small molecules, macromolecules, and particles.

Ga(III) as a chemical element presents a unique advantage over other radionuclides as it has properties closely resembling those of Fe(III) which is involved in many biochemical processes including inflammation. Moreover, Fe(III) is an essential nutrient and limiting factor of microbial life [98]. Stable Ga(III) has been used in treatment of various diseases including cancer, infection, and inflammation [99–101]. The ability of Ga(III) to bind iron proteins, for example, lactoferrin and transferrin as well as siderophores, and enzymes can be utilized in the imaging agent development.

4. Biomarkers and Radiopharmaceutical Development

The development of imaging agents relies strongly on the advances, experience, and knowledge of the research of biomarkers, for example, receptors and antigens; transport systems; substances involved in angiogenesis, glycolysis, hypoxia, proliferation, and apoptosis; and enzyme activity. Targeting biomarkers that are specific for a given disease is one the major aims of an agent development for both diagnostic imaging and therapy. The knowledge and access to respective vector molecules have considerably expanded due to the achievements in proteomics and genomics. Infection, inflammation, and fibrosis are closely interrelated processes and corresponding biomarkers might present practical interest in developing respective imaging agents. Favorable characteristics of a target in general include expression upregulation, absence of expression in normal tissue, and internalization or stable binding of the respective ligand for the longitudinal accumulation of the latter [102].

5. Imaging Inflammation

Inflammatory response is a complex process involving immune system cells (T- and B-lymphocytes, NK cells, macrophages, monocytes, neutrophils, eosinophils, and mast cells) and products of their (patho)physiological activity, for example, cytokines involved in the cell signaling. Various functions of the cells and their products as well as their receptors provide a broad range of potential imaging targets [103–107]. Targeting the white blood cells of the immune system such as macrophages, monocytes, lymphocytes, and neutrophils for the detection of their upregulation and trafficking, secretion of cytokines and chemokines, and phagocytosis has been investigated both clinically and preclinically. Receptors such as SSTR, NCA-90, integrins, folate, bombesin, vascular cell adhesion protein-1, and interleukins expressed by activated T-cells, CXCR2 expressed on neutrophils, and CXCR4 overexpressed by leukocytes have demonstrated potential for in vivo targeted imaging [108]. Respective ligands and substrates can be considered for radiolabelling. Cytokines including interferons, lymphokines, interleukins, and chemokines bind to various receptors, for example, IL1 and IL2 receptor types, IFN, CD40, CD37, CD30, CD4, CCR5, and IL1-17R receptor family. Folate, CD64, NCA90, and CD15 receptors expressed on macrophages, leukocytes, and granulocytes can serve as targets. Not only do molecules of such super families as chemokine, integrin, selectin, and immunoglobulin participate in the cell emigration cascade, but also enzymes on the surface of endothelia cells and leukocytes contribute to the leukocyte extravasation [109]. Receptors on the endothelial wall, for example, for binding of IL1 and TNFα, are another category of the targets. These are only few examples of targets for potential imaging agent development (Table 3). Many targets were utilized in oncology [28] and their translation to inflammation is feasible.

5.1. Targeting Cell Receptors with Antibodies. Radiolabelled (^{99m}Tc, ^{111}In, and ^{123}I) anti-CD2, anti-CD5, anti-CD25, anti-CD45 antibodies and their fragments were used for the imaging of T-lymphocyte infiltration in various inflammatory diseases [110]. Typically for antibody slow pharmacokinetics, the time delay between the administration and examination stretches up to 24 hours. Interleukin-8 labelled with ^{99m}Tc was studied in rabbits with induced acute pyogenic osteomyelitis [111] and induced acute colitis [112]. The agent was found suitable for the scintigraphic evaluation of the respective diseases. CD163 receptor expressed in monocytes and activated macrophages was targeted with an anti-CD163 antibody labelled with ^{68}Ga in rats with acute collagen-induced arthritis [45]. The agent demonstrated specific binding and thus potential for studies of inflammatory diseases.

5.2. Targeting Angiogenesis. Angiogenesis plays an important role in wound healing, chronic inflammation, and tumour growth [113]. The family of vascular endothelial growth factors (VEGF) and integrins play crucial role in the angiogenesis cascade. Integrin receptors are overexpressed on the surface of vascular endothelial cells during angiogenesis in malignances, tissue healing, and inflammation. The largest group is radiolabelled peptide ligands comprising arginine-glycine-aspartic acid (RGD) sequence and peptidomimetics targeting $\alpha_v\beta_3$ integrin receptors. Various analogues were developed introducing cyclization and multimerization; variety of chelate/coligand moieties; PKM such as carbohydrate and polyethylene glycol chains [114–121]. Various RGD analogues labelled with ^{18}F, ^{68}Ga, and ^{99m}Tc were used in oncological clinical trials [122]. The majority of them comprised ^{18}F; however, advantages of ^{68}Ga such as accessibility of the radionuclide, more straightforward and efficient labelling chemistry, lower radiation dose, and better image contrast rendered more extensive development of ^{68}Ga-based analogues [123–127].

The imaging agents tested in cancer systems can be relevant for the imaging of inflammation related diseases. The imaging and evaluation of synovial angiogenesis in patients with rheumatoid arthritis was accomplished using [^{68}Ga]Ga-PRGD$_2$ [46]. The elevated agent uptake was detected in the sites of active inflammation, rich neovasculature, and physiological integrin receptor expression, while no tracer accumulation was detected in axillary lymph nodes with reactive hyperplasia and strenuous skeletal muscles. [^{68}Ga]Ga-PRGD$_2$/PET-CT was found useful for the evaluation of synovial angiogenesis and follow-up of the treatment response.

[^{68}Ga]Ga-NOTA-c(RGDyK) was developed for the imaging of myocardial infarction (MI) and follow-up of the response to the therapeutic intervention and demonstrated promising results preclinically [47]. The uptake in the MI lesions was enhanced and correlated with the vascular endothelial growth factor expression. Dynamic [^{68}Ga]Ga-NOTA-c(RGDyK)/PET scanning with subsequent kinetic modeling studies in rats with forelimb ischemia showed higher uptake and distribution volume in the ischemic area as compared to that of sham operation and control regions [48]. Monitoring myocardial repair and angiogenesis after ischemic injury was found plausible using [^{68}Ga]Ga-NODAGA-RGD and [^{68}Ga]Ga-TRAP-(RGD)$_3$ in rat model [49]. Elevated uptake of [^{68}Ga]Ga-DOTA-E-[c(RGDfK)]$_2$ was observed in the infarcted area while no accumulation was detected in the noninfarcted myocardium of the same rats [50]. The uptake of [^{68}Ga]Ga-DOTA-RGD in atherosclerotic plaques was studied in vivo in atherosclerotic mice with promising results [52]. Elevated uptake of [^{68}Ga]Ga-NODAGA-RGD in injured myocardium as compared to viable ischemic areas in pig model presumably indicated increased expression of $\alpha_V\beta_3$ receptors associated with injury repair in the presence of coronary stenosis [51].

Although targeting VEGF receptors were studied in the context of cancerous diseases, chronic inflammation can also be considered. A ligand consisting of a single chain (scVEGF, 3–112 amino acids of human VEGF$_{121}$) [128, 129] was labelled with ^{68}Ga and the resulting agent showed distinct uptake in the tumour xenografts in mice; however high kidney uptake needed to be addressed [130, 131].

5.3. Targeting Selectins. P-selectin is expressed on the active endothelium surface and platelets and operates the migration of leukocytes in response to inflammatory cytokines.

Table 3: ^{68}Ga-based imaging agents for inflammation and infection investigated preclinically and clinically.

Target/mechanism	Imaging agent	Disease/microorganism (study type)
	Inflammation	
P-selectin	[^{68}Ga]Ga-Fucoidan	Atherosclerotic plaques (preclinical [44])
Anti-CD163	[^{68}Ga]Ga-anti-CD163-antibody	Acute collagen-induced arthritis (preclinical [45])
Integrins	[^{68}Ga]Ga-PRGD$_2$	Rheumatoid arthritis (clinical [46])
Integrins	[^{68}Ga]Ga-NOTA-c(RGDyK) [^{68}Ga]Ga-NODAGA-RGD [^{68}Ga]Ga-TRAP-(RGD)$_3$ [^{68}Ga]-DOTA-E-[c (RGDfK)]$_2$	Myocardial infarction (preclinical [47–51])
Integrins	[^{68}Ga]Ga-NODAGA-RGD	Atherosclerotic plaques (preclinical [52])
VAP-1	[^{68}Ga]Ga-Siglec	Synovial inflammation; inflammatory lung injury; atherosclerotic lesions; skin/muscle inflammation (preclinical [53–56])
VAP-1	[^{68}Ga]Ga-DOTAVAP-P1, [^{68}Ga]Ga-DOTAVAP-PEG-P1	Skin/muscle inflammation (preclinical [57])
CXCR4	[^{68}Ga]Ga-pentixafor	Ischemic heart; atherosclerotic plaques (clinical [58, 59])
FR	[^{68}Ga]Ga-DOTA-PEG-FA [^{68}Ga]Ga-DOTA-folate	Inflammation/implant (preclinical [60, 61])
SSTR	[^{68}Ga]Ga-DOTA-TOC	Sarcoidosis, idiopathic pulmonary fibrosis, Graves' disease, Hashimoto's disease, coronary artery plaque, atherosclerotic inflammation (clinical [62–65])
Mannose receptors	[^{68}Ga]Ga-NOTA-MSA	Myocarditis (preclinical [66])
Aβ plaques	^{68}Ga-labelled styrylpyridines, benzofuran, curcumin	Neuroinflammation, Alzheimer's disease (preclinical [67–69])
	Infection	
Antibiotics/inhibitor	[^{68}Ga]Ga-ciprofloxacin	*Staphylococcus aureus* (preclinical [70])
Antimicrobial/membrane	[^{68}Ga]Ga-NOTA-UBI29-41 [^{68}Ga]Ga-NOTA-UBI30-41	*Staphylococcus aureus* (preclinical [71, 72])
Antimicrobial/membrane	[^{68}Ga]Ga-DOTA-TBIA101	*E. coli* (preclinical [73, 74])
Antimicrobial/membrane	[^{68}Ga]Ga-GF-17 and [^{68}Ga]Ga-RAWVAWR-NH2	*E. coli* and *S. aureus* (preclinical [75])
Siderophores	[^{68}Ga]Ga-TAFC, [^{68}Ga]Ga-FC, [^{68}Ga]Ga-FOXE	Invasive pulmonary aspergillosis (preclinical [15, 16, 76])
Leukocytes	[^{68}Ga]Ga-citrate	Osteomyelitis, diskitis, intra-abdominal infection, tuberculosis, interstitial nephritis (clinical [18, 19, 77–80])
Leukocytes	[^{68}Ga]Ga-Apo-transferrin	*Staphylococcus aureus* (preclinical [14])

E-selectin binding peptide labelled with ^{99m}Tc accumulated in acute osteomyelitic lesions in rats presumably by interaction with activated vascular endothelium [132]. An analogue of P-selectin natural ligand, fucoidan, labelled with ^{68}Ga could discriminate active and inactive atheroschlerotic plaques in mice [44].

5.4. Targeting Vascular Adhesion Protein-1. Vascular adhesion protein-1 (VAP-1) and CD73 are endothelial surface enzymes involved in the recruitment of leukocytes and their movement from the blood into the tissue [109]. Endothelial activation that takes place during inflammation can be utilized for specific targeting imaging. Several peptide analogues

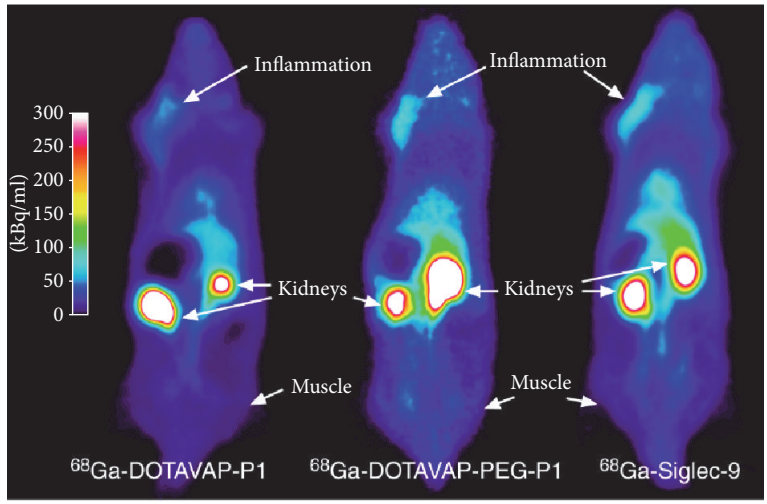

Figure 1: PET images of the distribution of [^{68}Ga]Ga-DOTAVAP-P1, [^{68}Ga]Ga-DOTAVAP-PEG-P1, and [^{68}Ga]Ga-DOTA-Siglec-9 in turpentine-induced rat model of sterile inflammation. All three peptide analogues showed target-to-nontarget ratio above 6 with rapid accumulation in the inflammation site and renal clearance. Adapted from [57].

labelled with ^{68}Ga were designed for the visualization of VAP-1 and showed promising results in animals with induced infection and sterile inflammation [7–13, 133]. The binding was proven specific and it was possible to differentiate inflammation from infection. [^{68}Ga]Ga-Siglec targeting VAP-1 demonstrated preclinical potential for imaging of synovial inflammation in patients with rheumatic diseases [53]. The same agent was utilized for respiratory distress syndrome (ARDS, an inflammatory lung injury) imaging in a porcine model [54]. Imaging VAP-1 with [^{68}Ga]Ga-Siglec was found promising also for the detection of inflamed atherosclerotic lesions [55] and inflammatory response induced by catheter implantation and staphylococcal infection [56]. ^{68}Ga-Siglec and two more peptide analogues with affinity to VAP-1 ([^{68}Ga]Ga-DOTAVAP-P1, [^{68}Ga]Ga-DOTAVAP-PEG-P1, and [^{68}Ga]Ga-DOTA-Siglec-9) were investigated in rat model of sterile skin/muscle inflammation (Figure 1) [57]. They showed distinct uptake in the affected sites.

5.5. Targeting Chemokines. Cytokines are produced by macrophages, B-lymphocytes, T-lymphocytes, and mast cells and act through receptors modulating, for example, immune response to infection and inflammation. Cytokines include chemokines, interleukins, interferons, and lymphokines that can be classified in broad families exhibiting diverse functions, for example, IL-1 and IL-6 superfamilies and TNF/TNF receptor superfamily. Therapeutics targeting cytokines are in clinical use, for example, inhibiting TNF or IL-6 in rheumatic diseases.

Chemokine receptors are physiologically expressed on B-lymphocytes, T-lymphocytes, macrophages, neutrophils, eosinophils, monocytes, and hematopoietic stem cells [134]. Imaging agents targeting CXCR4 are based on inhibitors (AMD3100) or small peptides (NFB, T140, pentixafor, and TN14003) and comprise ^{18}F, ^{67}Ga, ^{68}Ga, or ^{64}Cu [135–148]. They were developed and studied for the imaging of various cancerous diseases: lung, breast, prostate cancers, acute myeloid leukemia, and glioblastoma.

The application of CXCR4 targeting agents was extended beyond oncology. Clinical case/image reports [149, 150] were published on the utilization of [^{68}Ga]Ga-pentixafor for detection and quantification of CXCR4 receptor density in ischemic heart diseases reflecting the role of the receptor in inflammatory and progenitor cell recruitment [58, 59]. The same agent was successfully used in the assessment of macrophage infiltration in atherosclerotic plaques in rabbit disease model [151].

5.6. Targeting Folate Receptors. Folate receptors (FRs) are overexpressed on a variety of cancer cells and activated macrophages, but not on normal cells [152, 153]. The enhanced expression of FR was found in lung macrophages during acute inflammation [154]. The majority of the nuclear imaging agents based on folic acid or pteroic acid [155] were developed for diagnosis of cancers overexpressing FR receptors such as breast, cervical, ovarian, colorectal, nasopharyngeal, renal, and endometrial cancers. Various ^{68}Ga-labelled agents demonstrated accumulation in cell cultures and mice bearing folate-receptor positive human nasopharyngeal carcinoma cell line (KB) xenografts [6, 156–162]. [^{68}Ga]Ga-DOTA-PEG-FA comprising folic acid was investigated for the detection and quantification of inflammatory response to medical implants using mice with subcutaneously implanted polylactic acid and poly(N-isopropylacrylamide) particles as a model [60]. The agent was accumulated in the area of the implant most probably reflecting interaction of [^{68}Ga]Ga-DOTA-PEG-FA with folate receptor expressed on activated macrophages. Another folic acid based agent, [^{68}Ga]Ga-DOTA-folate, was successfully tested in an inflammatory paw rat model (Figure 2) [61]. Distinct accumulation in inflamed hand and foot joints of rheumatoid arthritis of a ^{99m}Tc-labelled folate analogue was observed in a patient, while no

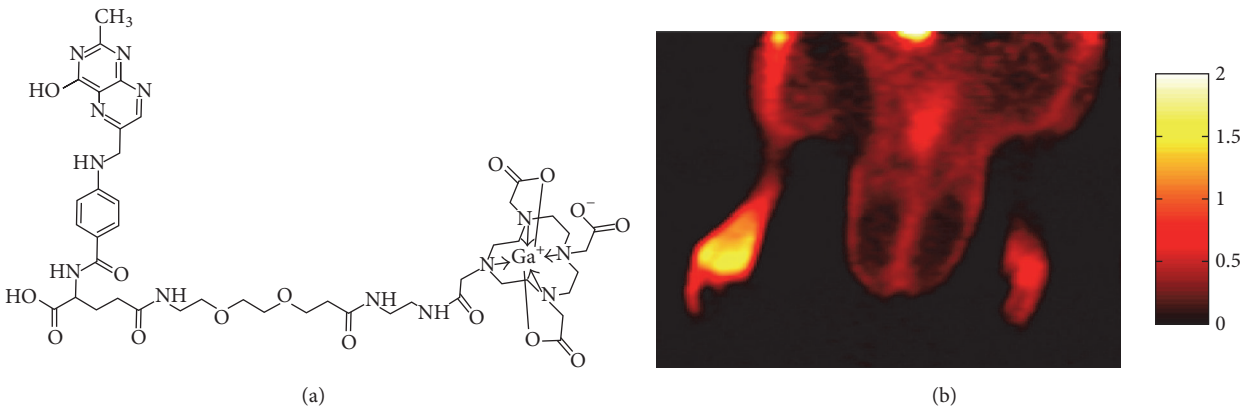

(a) (b)

Figure 2: Accumulation of [^{68}Ga]Ga-DOTA-folate (a) in the site of inflammation of rat inflammatory paw model induced by subcutaneously injected Complete Freund's Adjuvant (b). Adapted from [61].

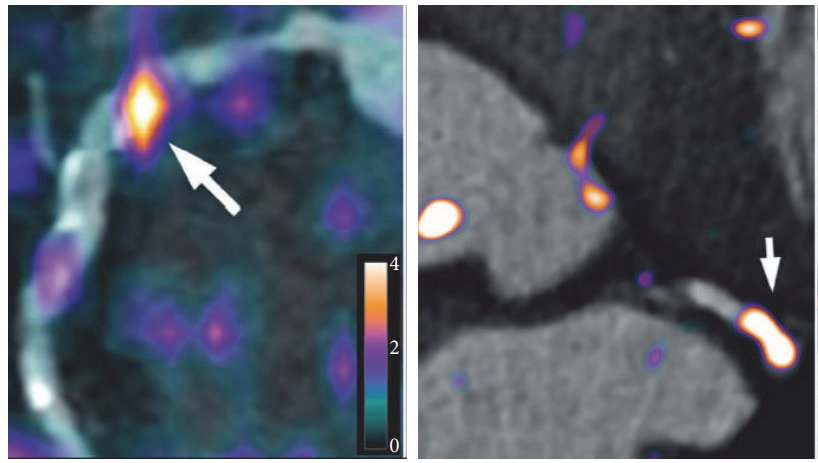

Figure 3: Intense atherosclerotic inflammation (white arrows) was detected by [^{68}Ga]Ga-DOTA-TATE in a patient with acute coronary syndrome. Adapted from [65].

uptake was detected in a nonarthritis patient's hands and feet [163].

5.7. Targeting Somatostatin Receptors. Somatostatin receptor (SSTR) ligand analogues have found an extensive application in diagnosis and radiotherapy of neuroendocrine tumours. The elevated expression of SSTRs is known also in small cell lung cancer, breast cancer, renal cell carcinoma, prostate cancer, and malignant lymphoma. A number of somatostatin ligand analogues labelled with gamma- and positron-emitting radionuclides were used clinically for oncological cases [85, 164–174]. ^{68}Ga-labelled somatostatin analogues demonstrated superior performance in terms of higher specificity and sensitivity, detection rate, shorter examination time, and quantification possibility and have become a golden standard for the detection of neuroendocrine tumours (NETs) taking over that title from [^{111}In]-pentetreotide (OctreoScan®) and demonstrating specificity and sensitivity of over 90% [27, 175–180]. ^{68}Ga-labelled agents for the imaging of NETs demonstrated advantages also over other radionuclides and tracers such as [^{18}F]FDG [174], ^{123}I-metaiodobenzylguanidine ([^{123}I]MIBG) [181, 182], [^{18}F]DOPA [183], [^{99m}Tc]-dicarboxy propane diphosphonate [184], and [^{18}F]NaF.

SSTR are also overexpressed on activated macrophages and T-lymphocytes. ^{68}Ga-labelled analogues were used in inflammation related diseases such as idiopathic pulmonary fibrosis [62], Graves' and Hashimoto's diseases [63], coronary artery plaque imaging and characterization [64], and atherosclerotic inflammation with excellent macrophage specificity (Figure 3) [65]. Promising diagnostic potential of a ^{99m}Tc-labelled analogue was demonstrated in patients with rheumatoid arthritis and secondary Sjogren's syndrome, and the method was suggested for the assistance in anti-TNF alpha antibody treatment planning [185]. [^{68}Ga]Ga-DOTA-TOC/PET-CT was found superior to ^{67}Ga-Citrate/SPECT in detection of sarcoidosis lesions [186]. A clinical study demonstrated correlation between uptake of [^{68}Ga]Ga-DOTA-TOC and SST_2 mRNA expression and recorded the information in a database [187] providing tools for accurate quantification

and evaluation of disease progression and treatment response in cancerous and inflammatory diseases involving SSTRs. Preclinical study using atherosclerotic mice demonstrated superior targeting properties of [^{68}Ga]Ga-DOTA-NOC as compared to [^{18}F]FDR-NOC [188], overall confirming the potential of SSTR targeting for atherosclerotic plaque imaging.

5.8. Imaging Neuroinflammation. Despite difficulty of designing ^{68}Ga-labelled molecules capable of blood-brain barrier penetration, several agents were suggested for the imaging of neuroinflammation, in particular Aβ plaques deposited on blood vessels [67–69]. Bivalent styrylpyridines labelled with ^{68}Ga demonstrated high specificity and affinity for Aβ plaques using postmortem Alzheimer's disease (AD) brain sections [67]. Benzofuran derivative comprising ^{68}Ga showed promising results in terms of binding specificity and affinity investigated in vitro in sections of Tg2576 mice [68]. Although the synthesis of a ^{68}Ga-labelled Pittsburgh compound analogue was successful, the in vitro binding to amyloid deposits was limited [69]. The common disadvantage of these agents is poor blood-brain barrier penetration; nevertheless the exploration of more successful analogues continues. Curcumin functions as an antioxidant, antimicrobial, anti-inflammatory, and anticancer agent. Diacetyl-curcumin and bis(dehydroxy)curcumin labelled with ^{68}Ga demonstrated in vitro binding to β-amyloid fibrils and lung cancer cells [189]. Potential application of the agents could include diagnostic imaging of Alzheimer's disease and various cancers.

6. Imaging Infection

Infection imaging can be indirect utilizing targets involved in the immune response, namely, inflammation, as presented in the inflammation targets section above or direct utilizing pathogen related targets. The direct imaging is especially crucial in cases where inflammatory response is absent. The difference in biochemistry and structure between bacterial and human cells might exclude physiological uptake by human tissue making it easier to meet the favorable characteristics of an imaging agent. However, discrimination between the various infectious microorganisms, pathogenic bacteria, and microbiota, targeting specific bacteria type as well as difficulty of accessing bacteria aggregated in a biofilm makes the task very challenging [190, 191]. The specific targeting of infection would require accumulation of the radioactive signal in the pathogen. The radiolabelled targeting agents for infection can be roughly divided into several groups: antibiotics based; antimicrobial protein and peptide based; siderophore and other metabolisable compound based; and antigen-specific antibodies and antibody fragments (Table 3).

6.1. Radiolabelled Antibiotics. Antimicrobials act on the processes that are specific to microbes, for example, bacteria and fungi, and thus corresponding imaging agents might distinguish infection from inflammation [191]. They might require internalization or may bind to the cell surface dependent on their biological action mechanism [191–193]. The possibility of antibiotic resistance development exists also in the case of imaging agents even though the amount of such agents would be subnanomolar [194, 195]. Another complication is possible nonspecific uptake of antibiotics based agents by leucocytes [196]. Considerable number of various antibiotic analogues have been labelled with ^{99m}Tc, ^{111}In, ^{131}I, ^{11}C, and ^{18}F [102] and evaluated preclinically and clinically with ^{99m}Tc-ciprofloxacin becoming a commercial product (Infecton) [21, 197, 198]. However, the further improvement of specificity is desirable [191]. Antibiotics are accessible and cheap, and they demonstrate high sensitivity [102, 191] making the development of ^{68}Ga-labelled analogues very attractive given the earlier mentioned advantages that ^{68}Ga as a radionuclide in combination with PET provides. Two ^{68}Ga-labelled analogues based on ciprofloxacin demonstrated potential for discrimination between bacterial infection and inflammation in rats infected with *Staphylococcus aureus* [70].

6.2. Radiolabelled Antimicrobial Proteins and Peptides. Antimicrobial proteins and peptides, for example, serprocidins, cathelicidins, and defensins produced by the cells of immune system, target microbial membrane lipids and impose microbicidal effect [35, 43]. They present a large group of potential candidates for microbial imaging including bacteria, fungi, parasites, and viruses. Antimicrobial peptides have demonstrated higher specificity for infection than antibiotic analogues. They accumulate at infection but not sterile inflammation sites. The most thoroughly studied antimicrobial peptide, ubiquicidin UBI [29–41] labelled with ^{99m}Tc [199], demonstrated promising results in human clinical trials [200, 201]. It has the potential for quantification of viable infecting microorganisms and consequently for monitoring the efficacy of antimicrobial therapy in patients.

Fragments of an antimicrobial peptide ubiquicidin conjugated to NOTA and labelled with ^{68}Ga, [^{68}Ga]Ga-NOTA-UBI29-41, and [^{68}Ga]Ga-NOTA-UBI30-41 demonstrated possibility for the distinction between infection and inflammation in a rabbit model [71, 72]. Antimicrobial peptide fragments GF-17 and RAWVAWR-NH2 of, respectively, human cathelicidin LL-37 and human lysozyme active against *E. coli* and *S. aureus* were labelled with ^{68}Ga and their biodistribution in normal rats demonstrated fast clearance from liver [75]. Antimicrobial depsipeptide based agent, [^{68}Ga]Ga-DOTA-TBIA101, targeting bacterial lipopolysaccharides detected muscular *E. coli*-infection in mice (Figure 4) [73]. The agent was also studied in healthy rabbits and various disease model rabbits such as sterile inflammation, *Staphylococcus aureus* infection, and *Mycobacterium tuberculosis* [74]. The clearance of [^{68}Ga]Ga-DOTA-TBIA101 from blood and normal tissue was fast, and enhanced uptake in sterile inflammation and *Mycobacterium tuberculosis* sites was observed. The improvement of the bacterial selectivity will require modification of the agent structure.

6.3. Radiolabelled Siderophores. Bacteria and fungi produce various siderophores for harvesting iron which is essential for their survival and growth [34, 98, 191]. Siderophores

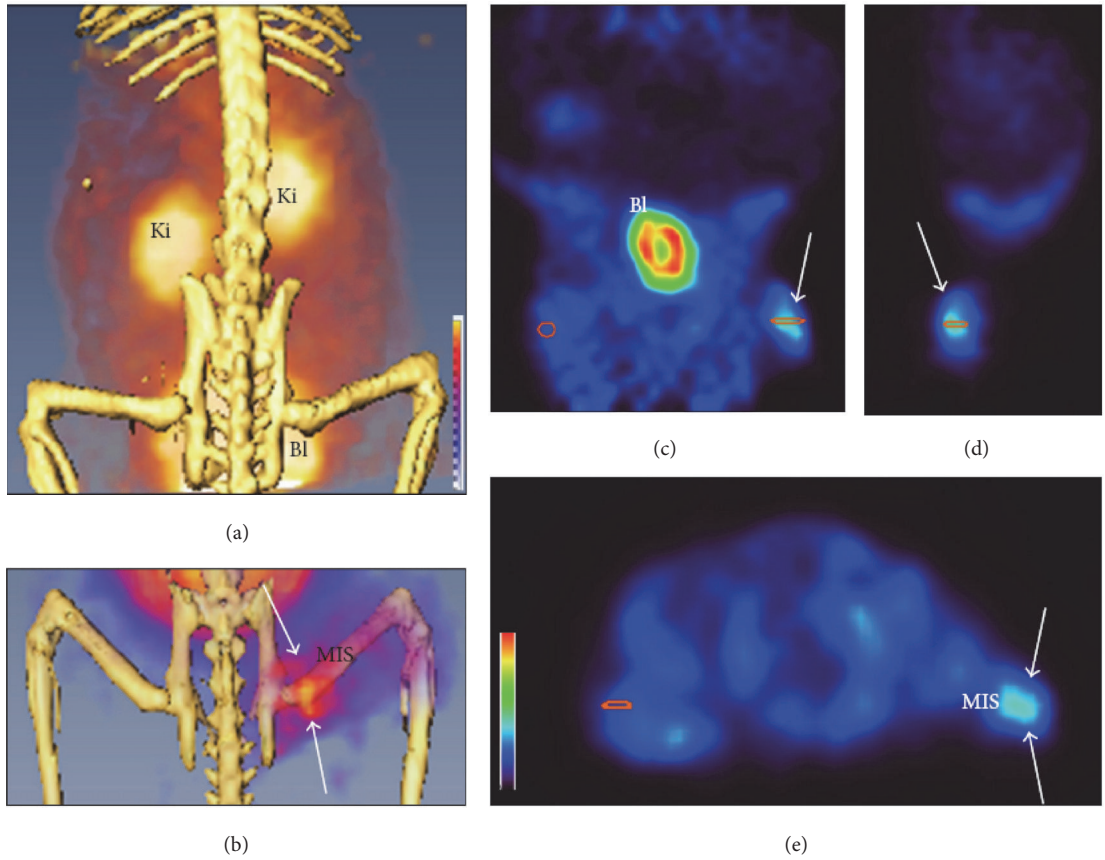

Figure 4: Left panel presents maximum intensity projection images of [^{68}Ga]Ga-DOTA-TBIA101 distribution in a healthy mouse (a) and a mouse with muscular infection site (MIS) in the right hind muscle tissue (white arrows). Right panel presents coronal (c), sagittal (d), and axial (e) images with uptake in the MIS (white arrow) and absence of the uptake in the contralateral muscle tissue. Ki and Bl stand, respectively, for kidney and bladder. Reproduced from [73].

can also play a critical role in the development of biofilms by microbes. They are low molecular weight compounds specifically chelating Fe(III), and Ga(III) can form stable complexes with them mimicking Fe(III) [202, 203].

Desferri-triacetylfusarinine C (TAFC) and desferri-ferricrocin (FC) labelled with ^{68}Ga were used for the imaging of invasive pulmonary aspergillosis (IPA) caused by Aspergillus *fumigatus* [15]. [^{68}Ga]Ga-TAFC demonstrated superior characteristics in terms of specific target binding, metabolic stability, and fast blood clearance in a rat model of *A. fumigatus* infection. Seven analogues were developed in another study with TAFC and ferrioxamine E (FOXE) showing favorable binding, clearance, elimination, and stability characteristics [16] as well as lung uptake in rat of invasive aspergillosis model wherein the uptake extent was correlated with disease severity [17]. [^{68}Ga]Ga-triacetylfusarinine C and [^{68}Ga]Ga-ferrioxamine E were investigated in rat model of *A. fumigatus* and demonstrated rapid uptake in the lungs (Figure 5) [76].

6.4. Radiolabelled Metabolisable Agents. Mammalian microbiota consumes (poly)saccharides, in particular maltose and maltodextrins [204]. The transport mechanism is specific to bacteria and is absent in mammalian cells making it possible to utilize these (poly)saccharides for imaging agent development. Maltodextrin functionalized with a fluorescent dye was internalized through the bacteria-specific maltodextrin transport pathway and discriminated between active bacteria and inflammation in vivo [192]. Maltose labelled with ^{18}F localized specifically bacterial infection in mice [205]. Potential to label polysaccharides directly with ^{68}Ga might be utilized extensively.

As mentioned above, the chemical properties of Ga(III) provide the potential for direct labelling of polysaccharides. Dextran was labelled directly and resulting complex demonstrated sufficient stability in human serum; however the feasibility of the bacterial imaging was not demonstrated [206].

Trapping of nucleosides that are substrates of thymidine kinase occurring within bacteria was explored using ^{18}F and ^{125}I labelled analogues of uracil [207]. Promising results were obtained in seven bacterial species in mice. Another study, in the context of therapeutic bacteria development, demonstrated possibility of detecting *Salmonella* vectors within tumours using ^{18}F-labelled uracil [208]. However,

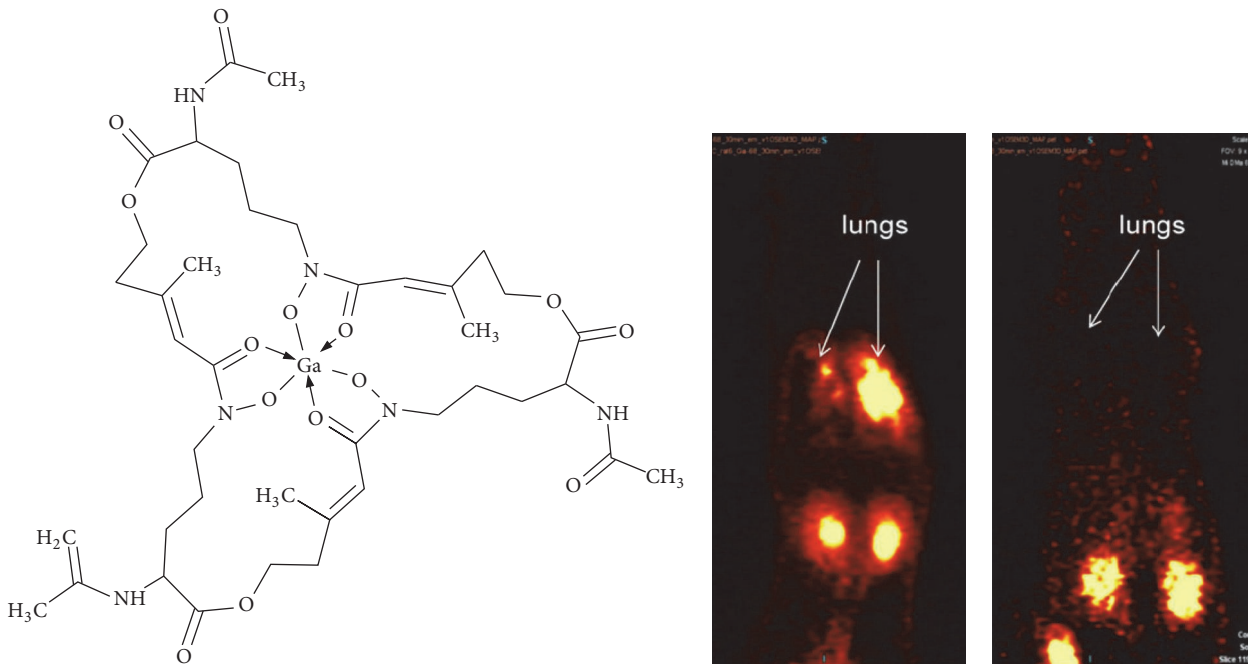

Figure 5: Molecular structure of [^{68}Ga]Ga-triacetylfusarinine C (a) used for the in vivo imaging of a rat with Aspergillus *fumigatus* infection (b) and negative control of noninfected rat (c). White arrows point at the infected (b) and normal (c) lungs. Adapted from [76].

the development of ^{68}Ga-labelled nucleosides that would maintain their biological activity is challenging and few examples known from the literature confirm that [4, 6].

7. ^{68}Ga-Citrate

As mentioned above ^{68}Ga/PET provides a number of advantages over ^{67}Ga/SPECT and following publications demonstrate it in clinical and preclinical studies. [^{68}Ga]Ga-citrate demonstrated high diagnostic accuracy of 90% of osteomyelitis and diskitis in clinical studies (Figure 6) [18, 19]. This study demonstrates that [^{68}Ga]Ga-citrate can be employed for monitoring the response to treatment. [^{68}Ga]Ga-citrate was used clinically to follow-up surgical intervention in patients with acute osteomyelitis and intra-abdominal infection [77]. The agent was also used to successfully visualize lung malignancy and tuberculosis in patients; however in case of high prevalence of granulomatous diseases the distinction between malignant and benign lung lesions was unclear [78, 79]. Another clinical study conducted head-to-head comparison of [^{68}Ga]Ga-citrate (Figure 7) and [^{18}F]FDG in patients with *Staphylococcus aureus* bacteremia [80]. The detection rate of osteomyelitis was similar, and further investigation of [^{68}Ga]Ga-citrate applicability in cases of osteomyelitis induced by other pathogens as well as for monitoring healing process is warranted.

Comparative study of [^{68}Ga]Ga-citrate and [^{67}Ga]Ga-citrate was performed in healthy and infection model rats [77]. The performance of [^{68}Ga]Ga-citrate was found superior in terms of image contrast in the lower abdomen and extremities. Potential of [^{68}Ga]Ga-citrate for the differentiation of acute interstitial nephritis from acute tubular necrosis was studied in rat model of the disease and it was demonstrated that the kidney uptake correlated with the extent of mononuclear cell infiltration accompanying inflammation [209]. ^{68}Ga-labelled *Apo*-transferrin demonstrated bacterial infection detection capacity in rat model with *Staphylococcus aureus* wherein the infection site was visualized 1 h after administration of the agent [14].

7.1. Radiolabelled Antibodies and Antibody Fragments. Human immunoglobulin (HIG) binds to bacteria but also accumulates at the sites of fungal and viral infection as well as sterile inflammation due to binding to leukocytes. The improved specificity for bacteria was achieved for the fragments of HIG. It is feasible to develop specific antibodies to various antigens present on the bacterial cell surface [102]. Monoclonal antibodies labelled with ^{99m}Tc were used for infection imaging via granulocytes targeting NCA-95 [210]. Various cytokines of interleukin family (IL-1, IL-8) labelled with ^{123}I or ^{99m}Tc demonstrated accumulation in the sites of infection in various animal models [111, 112, 211–214]. Registered antigranulocyte radiopharmaceuticals such as LeuTech®, Scintimun®, and Leukoscan® are based on ^{99m}Tc-labelled antibodies. This experience can be translated to ^{68}Ga; however either the size of the antibodies must be reduced or pretargeting techniques must be applied in order to overcome the discrepancy between the short physical half-life of ^{68}Ga and slow pharmacokinetics of antibodies.

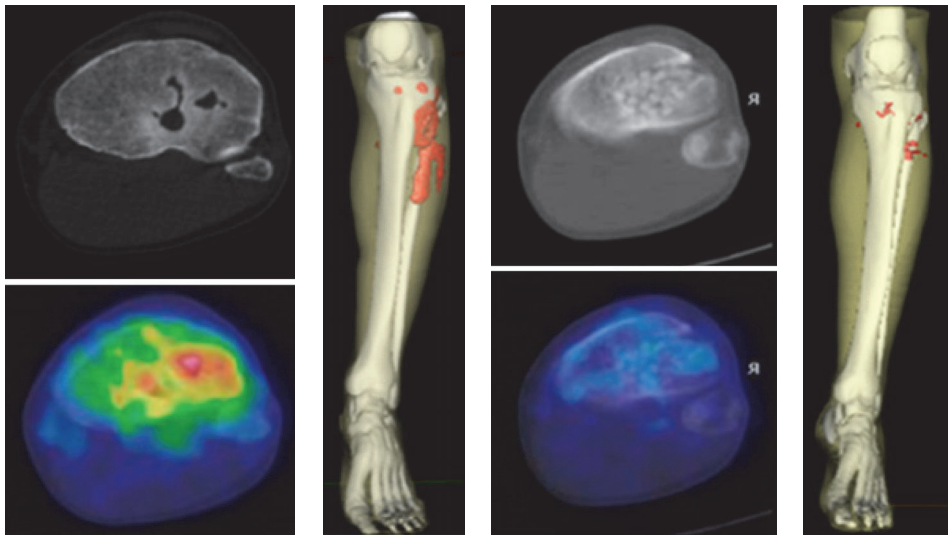

(a) (b) (c) (d)

Figure 6: [^{68}Ga]Ga-citrate PET/CT examination of a patient affected by acute osteomyelitis before (left panel) and after (right panel) surgical curettage showing uptake in the transaxial (a, c) and 3D reconstruction images (b, d; red area). Absence of the uptake after the therapy confirms complete response to the treatment. Adapted from [19].

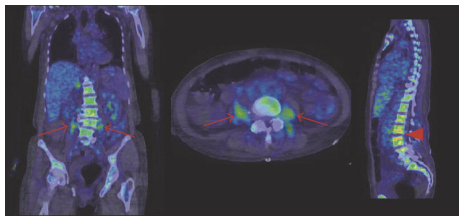

Figure 7: Vertebral osteomyelitis (spondylodiscitis; red arrowheads) and abscesses in the iliopsoas and paravertebral area (red arrows) were detected by [^{68}Ga]Ga-citrate in a patient admitted to the hospital with back pain and general symptoms. The PET acquisition was performed 88 min after administration of 245 MBq of [^{68}Ga]Ga-citrate. Adapted from [80].

7.2. Radiolabelled Biotin. Biotin is a growth factor utilized in many bacteria. An ^{111}In-labelled analogue of biotin was successfully utilized for diagnosis of vertebral infections in a clinical study [215]. It would be rational to explore the relevance of ^{68}Ga-labelled analogues given the advantages of ^{68}Ga over ^{111}In and promising [^{68}Ga]Ga-DOTA-Biotin analogues [216, 217] developed for monitoring survival of transplanted avidin-coated islets.

8. Miscellaneous

Stable Ga(III) complex with thiosemicarbazones demonstrated antimicrobial effect against *P. aeruginosa* and *C. albicans* due to most probably both displacement of essential Fe(III) with Ga(III) and thiosemicarbazones [101]. Substitution of the stable Ga(III) by radioactive ^{68}Ga might result in a specific infection imaging agent.

Selective imaging of Enterobacteriaceae using 2-[^{18}F]-fluorodeoxysorbitol (^{18}F-FDS) was demonstrated in a murine myositis model [218]. The uptake of ^{18}F-FDS was correlated with bacterial burden; moreover the agent differentiated infection from sterile inflammation. Given the potential of ^{68}Ga for the labelling of small biologically active molecules [4] it might be plausible to develop a respective analogue with added value of the advantages that ^{68}Ga offers including simpler production chemistry, lowered radiation dose, repetitive examination, and accessibility at clinical centers without cyclotrons and remote from [^{18}F]-FDG distribution sites. As mentioned above, the poor access to bacteria aggregated in a biofilm might make the imaging task challenging. Several peptide candidates with affinity for S. aureus biofilm were designed and labelled with ^{68}Ga [219]. The resulting agents demonstrated binding in vitro; however it was not possible to block the binding with excess of the cold peptide.

Ionic ^{68}Ga was found superior to [^{18}F]-FDG in infection detection in the rat model with diffuse osteomyelitis [220]. In another study, the uptake of ionic ^{68}Ga was observed in the aortic plaques of atherosclerotic mice, specifically at the sites rich in macrophages [221]. However, the slow blood clearance of ionic ^{68}Ga presents a limitation.

Chronic inflammation is the major reason of fibrosis [222]. ^{68}Ga-labelled SST analogue ([^{68}Ga]Ga-DOTA-NOC) demonstrated uptake in pathogenic areas in patients affected by idiopathic pulmonary fibrosis with potential for monitoring response to treatment and drug development [62]. Another clinical study using [^{68}Ga]Ga-pentixafor also showed potential of the agent for monitoring disease activity and response to treatment in idiopathic pulmonary fibrosis [223]. Peptide based agents, CNO2A-PEG$_2$-c[CPGRVMHGLHLGDDEGPC] and [^{68}Ga]Ga-NODAGA-PEG$_2$-c[CPGRVMHGLHLGDDEGPC] for the imaging and quantification of fibrosis by PET were developed and characterized preclinically showing fast clearance from normal

tissue and blood and binding specificity [89]. Dosimetry calculations demonstrated possibility of six examinations per year in humans assuring disease monitoring in longitudinal studies and routine clinical setup [224].

Several hyaluronan conjugates of oligonucleotides targeting CD44 positive cells were developed and tested in healthy rats, sham-operated rats, and rats with myocardial infarction [225]. The uptake of the agents was higher for the latter group and varied dependent on the difference in the oligonucleotide structure.

TLR2 and TLR4 expression levels in neutrophils were found higher in individuals with bacterial and viral infections than those in control samples. There is a possibility that IL-4, IL-8, IL-10, IL-12, and TNF-a might serve as biomarkers for infections and that IL-2, IL-8, or IL-10 is potentially able to distinguish between bacterial and viral infections [22].

Mannosylated human serum albumin labelled with ^{68}Ga via NOTA chelator moiety ([^{68}Ga]Ga-NOTA-MSA) was tested in a rat model of myocarditis targeting mannose receptors expressed on macrophages infiltrating myocardium [66]. The uptake in the diseased myocardium was considerably higher than that of the normal one and it was precluded by administration of excess of nonlabelled MSA indicating binding specificity. The tracer build-up was also observed in the organs of macrophage accumulation.

[^{68}Ga]Ga-DOTA was investigated for the quantification of increased blood flow which is one of the key events in inflammation [226]. The uptake kinetics of [^{68}Ga]Ga-DOTA in the site of inflammation in rats with induced inflammation correlated well with that of ^{15}O-water, suggesting high relevance [^{68}Ga]Ga-DOTA.

9. Pretargeted Imaging

The half-life of ^{68}Ga is shorter than that of ^{64}Cu, ^{67}Ga, ^{99m}Tc, ^{89}Zr, ^{111}In, and ^{123,124,125}I and thus in contrast to the latter it is not compatible with slow pharmacokinetics of large molecules such as antibodies and glycoproteins. The range of antigen-specific antibodies relevant to inflammation and infection is broad and a number of ^{99m}Tc-labelled antibodies were used clinically [20, 21, 227]. The respective range of ^{68}Ga-based agents could be similar. The solution to overcome the incompatibility of half-life time frames could be either the reduction of the antibody size or the application of the pretargeting concept.

The history of the pretargeting concept spans three decades, predominantly in the field of oncology [228–230]. It was developed to improve image contrast and dosimetry in immunoimaging and radioimmunotherapy when using radiolabelled antibody ligands with slow pharmacokinetics [231]. The arsenal of antibodies is vast and diverse encouraging extensive investment into development of techniques that would allow their exploration to the fullest. Pretargeting considers at least two major steps wherein a functionalized antibody is first administered for target localization and clearance from blood and normal tissue and thereafter a radiolabelled small molecule capable of binding to the functionalized antibody due to high affinity or covalent interaction is administered. The key properties of the radiolabelled molecules are fast pharmacokinetic and clearance. Several techniques have been developed for the realization of pretargeting concept including avidin/streptavidin-biotin systems [216, 217, 232, 233]; bispecific antibodies (bsmAb) with haptens [232, 234–254]; antibody-oligonucleotide conjugates with complementary oligonucleotides [255]; biorthogonal systems allowing covalent chemical reactions in vivo (Figure 8).

The high affinity of biotin to avidin and streptavidin proteins was utilized clinically and preclinically in pretargeting approach for the imaging and therapy of pancreatic adenocarcinoma [232], glioblastoma [256], and lymphoma [257]. However, this pretargeting technique may require three steps in order to eliminate the excess of antibody-(strept)avidin conjugate, circulating in the blood and not bound to the target, by adding clearing agent. Another application of the technique was monitoring transplantation of islets of Langerhans in the treatment for type 1 diabetes mellitus, wherein the cells or cell mimetics were conjugated to (strept)avidin prior to the transplantation [216, 217]. Several analogues of biotin comprising DOTA chelate moiety for labelling with ^{68}Ga and ethylene glycol linker of various length demonstrated the influence of the latter on the affinity towards avidin.

Particular example of hapten molecules is the ones comprising histamine-succinyl-glycine (HSG) motif and chelate moiety [251–253, 258] for the complexation with ^{68}Ga. Several analogues were developed for the imaging of carcinoembryonic antigen (CEA) pretargeted with anti-CEA bsmAb [254, 259, 260], and two clinical studies of medullary thyroid carcinoma and breast carcinoma positive for CEA using ^{68}Ga-labelled hapten molecules and bsmAb were initiated [261].

Bioorthogonal reactions are fast, regioselective, requiring small reagent concentration, and occurring under mild conditions often in aqueous solution and temperature below 37°C [262, 263]. Amongst various biorthogonal reaction types, the cycloaddition of tetrazines and various dienophiles referred to as inverse-electron-demand Diels-Alder (IEDDA) reaction is the most successful in the context of pretargeting. Antibodies functionalized with *trans*-cyclooctene (TCO) and a radiolabelled tetrazine that can interact in vivo based on IEDDA reaction were studied [264–267]. In particular, ^{68}Ga-labelled tetrazine dextran demonstrated favorable pharmacokinetics in a healthy mouse [264]. However, the proof of concept is to be performed in a xenografted animal. Accumulation of anti-TAG72 [265] and anti-A33 [266] antibodies functionalized with TCO in mouse xenografts was visualized, respectively, by an ^{111}In and ^{64}Cu-labelled tetrazine analogues. Anti-CA19.9 antibody-TCO in combination with ^{177}Lu-labelled tetrazine demonstrated radiotherapeutic effect in pancreatic cancer murine model [267].

The pretargeted imaging techniques may contribute to the expansion of immuno-PET with ^{68}Ga providing the intrinsic advantages of ^{68}Ga and PET. As mentioned above, most of the developed radiolabelled counterparts of pretargeting techniques have demonstrated promising results. There are

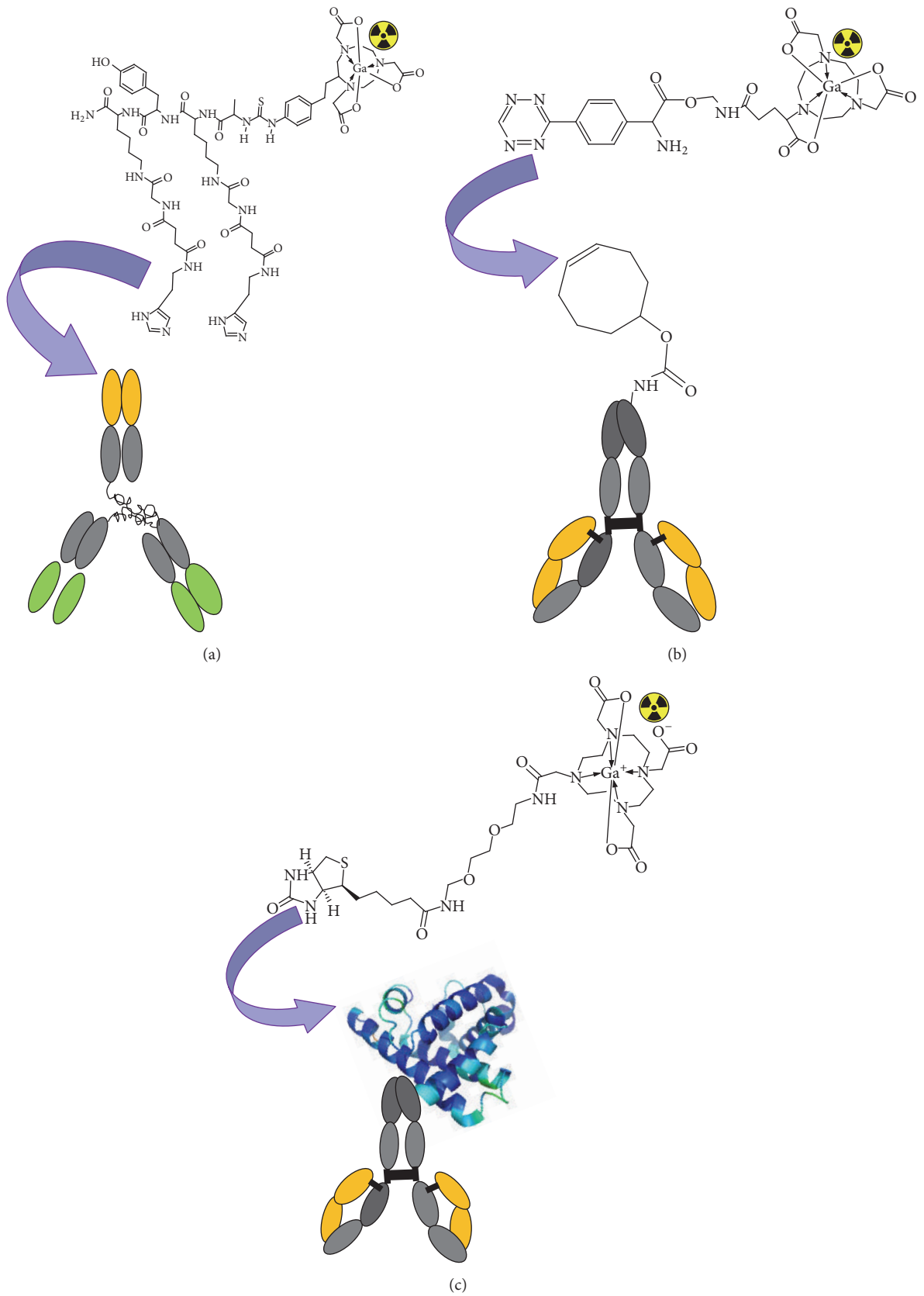

Figure 8: Schematic presentation of pretargeting techniques: (a) bispecific antibodies engineered to specifically bind with radiolabelled hapten molecules; (b) bioorthogonal click chemistry for fast and specific covalent binding between, for example, a *trans*-cyclooctene functionalized antibody and a radiolabelled tetrazine; (c) interaction between antibody-(strept)avidin conjugate and radiolabelled biotin utilizing extremely high affinity of (strept)avidin and biotin.

a considerable number of potential antibody biomarkers that could be considered for the imaging of infection and inflammation.

10. Theranostics Potential

Theranostics [268] embraces realization of personalized medicine by conducting diagnosis on individual basis and providing possibility of predicting the efficacy of a specific treatment and following up the response to the treatment enabling adjustment of the latter very early in the process. In the context of nuclear medicine wherein the radiopharmaceuticals targeted at biomarkers specific to a disease can carry either diagnostic radionuclides or therapeutic ones, the concept can be denoted as radiotheranostics [28]. The targeted molecular imaging such as PET can offer noninvasive diagnosis specific to the disease, for example, tumour-type specific, and provide accurate localization of the lesions. The strongest advantage of PET is the potential for quantification of the target, for example, receptor expression, investigation of the uptake kinetics, and estimation of the dosimetry. These characteristics of PET allow for individualized treatment selection and planning, monitoring of treatment response, and detection of recurrent disease. The individualized patient management provides such advantages as optimization of the treatment regimen for the improved response and exclusion of futile treatments, minimization of risks and toxicity with overall outcome of reduced cost and patient distress. The importance of individualized patient management was demonstrated by clinical studies wherein the influence of dose of the administered radiopharmaceutical, targeted at receptors overexpressed in cancer lesions, on the diagnostic outcome was investigated in the same patient [85, 269, 270]. ^{68}Ga-labelled SST analogues [26–28, 271] and Affibody molecules [5, 272–274] used, respectively, in NENs and breast cancer patients are the most prominent examples of (radio)theranostics involving ^{68}Ga/PET wherein ^{68}Ga-labelled analogues were used not only for localization of the lesions, but also for staging, patient stratification, prognosis, therapy selection, and monitoring of the response to the treatment of NETs and other cancer types [2–4, 6, 85, 176, 275–277].

The methodology can be translated to inflammation and infection allowing for accurate and specific selection of treatment regimen and for follow-up and evaluation of the response to therapy, resulting in improved treatment efficacy and decreased cost and side effects. The accommodation of both imaging function and antibiotic function in the same molecule is a novel example of a theranostic agent [278]. A series of siderophores conjugated with DOTA moiety for the radiolabelling and with antibiotics for the treatment of bacterial infection were investigated preclinically. The accumulation of the intravenously administered ampicillin conjugate in the site of subcutaneously injected *P. aeruginosa* in mice was clearly and focally visualized within 0.6 h with retention for at least 24 h. These results obtained using analogues carrying dye for optical imaging can be translated to ^{68}Ga-labelled counterparts for PET.

11. Conclusions

The medical need for specific agents for noninvasive, quantitative, and whole-body imaging of inflammation and infection has not been met yet despite decades of research. However, the prerequisites in terms of identification of potential targets, design and synthesis of the respective ligands, and imaging technologies are evolving very fast. The potential of accurate and quantitative lesion localization as well as monitoring of the treatment response promises personalized patient management.

The use of ^{68}Ga in oncology is established proving the strong potential of ^{68}Ga for the promotion of PET technology for effective and efficient diagnostics and personalized medicine. The experience of oncological ^{68}Ga-based agents is getting translated to inflammation and infection. Pretargeted imaging technology opens wide possibilities based on antibody biomarkers.

Conflicts of Interest

The author declares that there are no conflicts of interest regarding the publication of this article.

References

[1] I. Velikyan, "Continued rapid growth in Ga applications: update 2013 to June 2014," *Journal of Labelled Compounds & Radiopharmaceuticals*, pp. 99–121, 2015.

[2] I. Velikyan, "^{68}Ga-based radiopharmaceuticals: Production and application relationship," *Molecules*, vol. 20, no. 7, pp. 12913–12943, 2015.

[3] M. Fani, P. Peitl, and I. Velikyan, "Current status of radiopharmaceuticals for the theranostics of neuroendocrine neoplasms," *Pharmaceuticals*, vol. 10, no. 1, article no. 30, 2017.

[4] I. Velikyan, "Positron emitting [68Ga]Ga-based imaging agents: Chemistry and diversity," *Medicinal Chemistry*, vol. 7, no. 5, pp. 345–379, 2011.

[5] J. Sörensen, I. Velikyan, D. Sandberg et al., "Measuring HER2-receptor expression in metastatic breast cancer using [68Ga]ABY-025 Affibody PET/CT," *Theranostics*, vol. 6, no. 2, pp. 262–271, 2016.

[6] I. Velikyan, "Prospective of 68Ga-Radiopharmaceutical development," *Theranostics*, vol. 4, no. 1, pp. 47–80, 2014.

[7] P. Lankinen, T. J. Mäkinen, T. A. Pöyhönen et al., "68Ga-DOTAVAP-P1 PET imaging capable of demonstrating the phase of inflammation in healing bones and the progress of infection in osteomyelitic bones," *European Journal of Nuclear Medicine and Molecular Imaging*, vol. 35, no. 2, pp. 352–364, 2008.

[8] T. Ujula, M. Huttunen, P. Luoto et al., "Matrix metalloproteinase 9 targeting peptides: Syntheses, 68Ga-labeling, and preliminary evaluation in a rat melanoma xenograft model," *Bioconjugate Chemistry*, vol. 21, no. 9, pp. 1612–1621, 2010.

[9] A. Autio, T. Ujula, P. Luoto, S. Salomäki, S. Jalkanen, and A. Roivainen, "PET imaging of inflammation and adenocarcinoma xenografts using vascular adhesion protein 1 targeting peptide 68Ga-DOTAVAP-P1: Comparison with 18F-FDG," *European Journal of Nuclear Medicine and Molecular Imaging*, vol. 37, no. 10, pp. 1918–1925, 2010.

[10] J. Silvola, A. Autio, P. Luoto, S. Jalkanen, and A. Roivainen, "Preliminary evaluation of novel 68Ga-DOTAVAP-PEG-P2 peptide targeting vascular adhesion protein-1," *Clinical Physiology and Functional Imaging*, vol. 30, no. 1, pp. 75–78, 2010.

[11] T. Ujula, S. Salomäki, P. Virsu et al., "Synthesis, 68Ga labeling and preliminary evaluation of DOTA peptide binding vascular adhesion protein-1: a potential PET imaging agent for diagnosing osteomyelitis," *Nuclear Medicine and Biology*, vol. 36, no. 6, pp. 631–641, 2009.

[12] A. Autio, T. Henttinen, H. J. Sipilä, S. Jalkanen, and A. Roivainen, "Mini-PEG spacering of VAP-1-targeting 68Ga-DOTAVAP-P1 peptide improves PET imaging of inflammation," *EJNMMI Research*, vol. 1, no. 1, pp. 1–7, 2011.

[13] K. Aalto, A. Autio, E. A. Kiss et al., "Siglec-9 is a novel leukocyte ligand for vascular adhesion protein-1 and can be used in PET imaging of inflammation and cancer," *Blood*, vol. 118, no. 13, pp. 3725–3733, 2011.

[14] V. Kumar, D. K. Boddeti, S. G. Evans, F. Roesch, and R. Howman-Giles, "Potential use of ^{68}Ga-apo-transferrin as a PET imaging agent for detecting Staphylococcus aureus infection," *Nuclear Medicine and Biology*, vol. 38, no. 3, pp. 393–398, 2011.

[15] M. Petrik, H. Haas, G. Dobrozemsky et al., "68Ga-siderophores for PET imaging of invasive pulmonary aspergillosis: Proof of principle," *Journal of Nuclear Medicine*, vol. 51, no. 4, pp. 639–645, 2010.

[16] M. Petrik, H. Haas, M. Schrettl, A. Helbok, M. Blatzer, and C. Decristoforo, "In vitro and in vivo evaluation of selected 68Ga-siderophores for infection imaging," *Nuclear Medicine and Biology*, vol. 39, no. 3, pp. 361–369, 2012.

[17] M. Petrik, G. M. Franssen, H. Haas et al., "Preclinical evaluation of two 68Ga-siderophores as potential radiopharmaceuticals for Aspergillus fumigatus infection imaging," *European Journal of Nuclear Medicine and Molecular Imaging*, vol. 39, no. 7, pp. 1175–1183, 2012.

[18] A. Rizzello, D. Di Pierro, F. Lodi et al., "Synthesis and quality control of 68Ga citrate for routine clinical PET," *Nuclear Medicine Communications*, vol. 30, no. 7, pp. 542–545, 2009.

[19] C. Nanni, C. Errani, and L. Boriani, " ^{68}Ga-citrate PET/CT for evaluating patients with infections of the bone: preliminary results," *Journal of Nuclear Medicine*, vol. 51, no. 12, pp. 1932–1936, 2010.

[20] S. S. Das, A. V. Hall, D. W. Wareham, and K. E. Britton, "Infection imaging with radiopharmaceuticals in the 21st century," *Brazilian Archives of Biology and Technology*, vol. 45, no. spe, pp. 25–37, 2002.

[21] A. Signore and A. W. J. M. Glaudemans, "The molecular imaging approach to image infections and inflammation by nuclear medicine techniques," *Annals of Nuclear Medicine*, vol. 25, no. 10, pp. 681–700, 2011.

[22] T. Yusa, K. Tateda, A. Ohara, and S. Miyazaki, "New possible biomarkers for diagnosis of infections and diagnostic distinction between bacterial and viral infections in children," *Journal of Infection and Chemotherapy*, vol. 23, no. 2, pp. 96–100, 2017.

[23] A. Signore, A. W. J. M. Glaudemans, O. Gheysens, C. Lauri, and O. A. Catalano, "Nuclear Medicine Imaging in Pediatric Infection or Chronic Inflammatory Diseases," *Seminars in Nuclear Medicine*, vol. 47, no. 3, pp. 286–303, 2017.

[24] I. Velikyan, "Molecular imaging and radiotherapy: Theranostics for personalized patient management," *Theranostics*, vol. 2, no. 5, pp. 424–426, 2012.

[25] F. Rösch and R. P. Baum, "Generator-based PET radiopharmaceuticals for molecular imaging of tumours: On the way to THERANOSTICS," *Dalton Transactions*, vol. 40, no. 23, pp. 6104–6111, 2011.

[26] R. P. Baum, H. R. Kulkarni, and C. Carreras, "Peptides and receptors in image-guided therapy: Theranostics for neuroendocrine neoplasms," *Seminars in Nuclear Medicine*, vol. 42, no. 3, pp. 190–207, 2012.

[27] R. P. Baum and H. R. Kulkarni, "Theranostics: From molecular imaging using Ga-68 labeled tracers and PET/CT to personalized radionuclide therapy - the bad berka experience," *Theranostics*, vol. 2, no. 5, pp. 437–447, 2012.

[28] I. Velikyan, "Radionuclides for Imaging and Therapy in Oncology," *Cancer Theranostics*, pp. 285–325, 2014.

[29] J. Czernin and W. A. Weber, "Issues and controversies in nuclear medicine. Introduction," *Journal of Nuclear Medicine*, vol. 52, no. Supplement 2, pp. 1S–2S, 2011.

[30] S. J. Goldsmith and S. Vallabhajosula, "Clinically proven radiopharmaceuticals for infection imaging: mechanisms and applications," *Seminars in Nuclear Medicine*, vol. 39, no. 1, pp. 2–10, 2009.

[31] M. F. Tsan, "Mechanism of gallium-67 accumulation in inflammatory lesions," *Journal of Nuclear Medicine*, vol. 26, no. 1, pp. 88–92, 1985.

[32] S. L. Kipper, "Radiolabelled leukocyte imaging of the abdomen," in *Nuclear Medicine Annual*, J. Freeman, Ed., pp. 81–126, Raven Press, New York, NY, USA, 1995.

[33] F. Jamar, J. Buscombe, A. Chiti et al., "EANM/SNMMI guideline for ^{18}F-FDG use in inflammation and infection," *Journal of Nuclear Medicine*, vol. 54, no. 4, pp. 647–658, 2013.

[34] C. J. Palestro, "The current role of gallium imaging in infection," *Seminars in Nuclear Medicine*, vol. 24, no. 2, pp. 128–141, 1994.

[35] M. S. Akhtar, M. B. Imran, M. A. Nadeem, and A. Shahid, "Antimicrobial peptides as infection imaging agents: better than radiolabeled antibiotics," *International Journal of Peptides*, vol. 2012, Article ID 965238, 19 pages, 2012.

[36] D. Delbeke and G. M. Segall, "Status of and trends in nuclear medicine in the United States," *Journal of Nuclear Medicine*, vol. 52, no. 2, 2011.

[37] S. S. Gambhir, J. Czernin, J. Schwimmer, D. H. Silverman, R. E. Coleman, and M. E. Phelps, "A tabulated summary of the FDG PET literature," *Journal of Nuclear Medicine*, vol. 42, pp. 1S–93S, 2001.

[38] M. J. Lindsay, B. A. Siegel, S. R. Tunis et al., "The National Oncologic PET Registry: Expanded Medicare coverage for PET under coverage with evidence development," *American Journal of Roentgenology*, vol. 188, no. 4, pp. 1109–1113, 2007.

[39] F. Gemmel, H. Van Den Wyngaert, C. Love, M. M. Welling, P. Gemmel, and C. J. Palestro, "Prosthetic joint infections: radionuclide state-of-the-art imaging," *European Journal of Nuclear Medicine and Molecular Imaging*, vol. 39, no. 5, pp. 892–909, 2012.

[40] J. Sörensen, "How does the patient benefit from clinical PET?" *Theranostics*, vol. 2, no. 5, pp. 427–436, 2012.

[41] S. L. Rice, C. A. Roney, P. Daumar, and J. S. Lewis, "The next generation of positron emission tomography radiopharmaceuticals in oncology," *Seminars in Nuclear Medicine*, vol. 41, no. 4, pp. 265–282, 2011.

[42] R. L. Wahl, J. M. Herman, and E. Ford, "The Promise and Pitfalls of Positron Emission Tomography and Single-Photon Emission Computed Tomography Molecular Imaging-Guided Radiation Therapy," *Seminars in Radiation Oncology*, vol. 21, no. 2, pp. 88–100, 2011.

[43] A. W. J. M. Glaudemans, R. H. J. A. Slart, J. M. Van Dijl, M. Van Oosten, and G. M. Van Dam, "Molecular imaging of infectious and inflammatory diseases: A terra incognita," *Journal of Nuclear Medicine*, vol. 56, no. 5, pp. 659–661, 2015.

[44] X. Li, W. Bauer, I. Israel et al., "Targeting p-selectin by gallium-68-labeled fucoidan positron emission tomography for noninvasive characterization of vulnerable plaques: Correlation with in vivo 17.6t mri," *Arteriosclerosis, Thrombosis, and Vascular Biology*, vol. 34, no. 8, pp. 1661–1667, 2014.

[45] S. Eichendorff, P. Svendsen, D. Bender et al., "Biodistribution and PET Imaging of a Novel [^{68}Ga]-Anti-CD163-Antibody Conjugate in Rats with Collagen-Induced Arthritis and in Controls," *Molecular Imaging and Biology*, vol. 17, no. 1, pp. 87–93, 2014.

[46] Z. Zhu, Y. Yin, K. Zheng et al., "Evaluation of synovial angiogenesis in patients with rheumatoid arthritis using 68Ga-PRGD2 PET/CT: A prospective proof-of-concept cohort study," *Annals of the Rheumatic Diseases*, vol. 73, no. 6, pp. 1269–1272, 2014.

[47] J. S. Eo, J. C. Paeng, S. Lee et al., "Angiogenesis imaging in myocardial infarction using 68Ga-NOTA- RGD PET: Characterization and application to therapeutic efficacy monitoring in rats," *Coronary Artery Disease*, vol. 24, no. 4, pp. 303–311, 2013.

[48] J. H. Kim, Y.-H. Kim, Y. J. Kim et al., "Quantitative positron emission tomography imaging of angiogenesis in rats with forelimb ischemia using 68Ga-NOTA-c(RGDyK)," *Angiogenesis*, vol. 16, no. 4, pp. 837–846, 2013.

[49] I. Laitinen, J. Notni, K. Pohle et al., "Comparison of cyclic RGD peptides for $\alpha v\beta 3$ integrin detection in a rat model of myocardial infarction," *EJNMMI Research*, vol. 3, no. 1, pp. 1–9, 2013.

[50] M. Kiugel, I. Dijkgraaf, V. Kytö et al., "Dimeric [^{68}Ga]DOTA-RGD Peptide Targeting α <inf>v</inf> β <inf>3</inf> Integrin Reveals Extracellular Matrix Alterations after Myocardial Infarction," *Molecular Imaging and Biology*, vol. 16, no. 6, pp. 793–801, 2014.

[51] M. Grönman, M. Tarkia, T. Kiviniemi et al., "Imaging of $\alpha v\beta 3$ integrin expression in experimental myocardial ischemia with [68Ga]NODAGA-RGD positron emission tomography," *Journal of Translational Medicine*, vol. 15, no. 1, p. 144, 2017.

[52] J. Haukkala, I. Laitinen, P. Luoto et al., "68Ga-DOTA-RGD peptide: Biodistribution and binding into atherosclerotic plaques in mice," *European Journal of Nuclear Medicine and Molecular Imaging*, vol. 36, no. 12, pp. 2058–2067, 2009.

[53] H. Virtanen, A. Autio, R. Siitonen et al., "68Ga-DOTA-Siglec-9 - a new imaging tool to detect synovitis," *Arthritis Research & Therapy*, vol. 17, no. 1, article no. 308, 2015.

[54] J. Retamal, J. Sorensen, M. Lubberink et al., "Feasibility of (68) Ga-labeled Siglec-9 peptide for the imaging of acute lung inflammation: a pilot study in a porcine model of acute respiratory distress syndrome," *Am J Nucl Med Mol Imaging*, vol. 6, no. 1, pp. 18–31, 2016.

[55] J. M. U. Silvola, H. Virtanen, R. Siitonen et al., "Leukocyte trafficking-associated vascular adhesion protein 1 is expressed and functionally active in atherosclerotic plaques," *Scientific Reports*, vol. 6, Article ID 35089, 2016.

[56] H. Ahtinen, J. Kulkova, L. Lindholm et al., "68Ga-DOTA-Siglec-9 PET/CT imaging of peri-implant tissue responses and staphylococcal infections," *EJNMMI Research*, vol. 4, no. 1, article no. 45, pp. 1–11, 2014.

[57] A. Autio, S. Jalkanen, and A. Roivainen, "Nuclear imaging of inflammation: Homing-associated molecules as targets," *EJNMMI Research*, vol. 3, no. 1, pp. 1–7, 2013.

[58] J. T. Thackeray, T. Derlin, A. Haghikia et al., "Molecular Imaging of the Chemokine Receptor CXCR4 after Acute Myocardial Infarction," *JACC: Cardiovascular Imaging*, vol. 8, no. 12, pp. 1417–1426, 2015.

[59] J. S. Schmid, A. Schirbel, A. K. Buck, S. Kropf, H.-J. Wester, and C. Lapa, "Pentixafor-Positron Emission Tomography/Computed Tomography Detects Chemokine Receptor CXCR4 Expression after Ischemic Stroke," *Circulation: Cardiovascular Imaging*, vol. 9, no. 9, Article ID e005217, 2016.

[60] J. Zhou, G. Hao, H. Weng et al., "In vivo evaluation of medical device-associated inflammation using a macrophage-specific positron emission tomography (PET) imaging probe," *Bioorganic & Medicinal Chemistry Letters*, vol. 23, no. 7, pp. 2044–2047, 2013.

[61] S. A. Kularatne, M.-J. Bélanger, X. Meng et al., "Comparative analysis of folate derived PET imaging agents with [18F]-2-fluoro-2-deoxy-d-glucose using a rodent inflammatory paw model," *Molecular Pharmaceutics*, vol. 10, no. 8, pp. 3103–3111, 2013.

[62] V. Ambrosini, M. Zompatori, F. De Luca et al., "68Ga-DOTANOC PET/CT Allows Somatostatin Receptor Imaging in Idiopathic Pulmonary Fibrosis: Preliminary Results," *Journal of Nuclear Medicine*, vol. 51, no. 12, pp. 1950–1955, 2010.

[63] T. Lincke, J. Singer, R. Kluge, O. Sabri, and R. Paschke, "Relative quantification of indium-111 pentetreotide and gallium-68 DOTATOC uptake in the thyroid gland and association with thyroid pathologies," *Thyroid*, vol. 19, no. 4, pp. 381–389, 2009.

[64] A. Rominger, T. Saam, E. Vogl et al., "In vivo imaging of macrophage activity in the coronary arteries using 68Ga-DOTATATE PET/CT: correlation with coronary calcium burden and risk factors," *Journal of Nuclear Medicine*, vol. 51, no. 2, pp. 193–197, 2010.

[65] J. M. Tarkin, F. R. Joshi, N. R. Evans et al., "Detection of Atherosclerotic Inflammation by ^{68}Ga-DOTATATE PET Compared to [^{18}F]FDG PET Imaging," *Journal of the American College of Cardiology*, vol. 69, no. 14, pp. 1774–1791, 2017.

[66] S.-P. Lee, H.-J. Im, S. Kang et al., "Noninvasive imaging of myocardial inflammation in myocarditis using 68Ga-tagged mannosylated human serum albumin positron emission tomography," *Theranostics*, vol. 7, no. 2, pp. 413–424, 2017.

[67] Z. Zha, J. Song, S. R. Choi et al., "68Ga-Bivalent Polypegylated Styrylpyridine Conjugates for Imaging Aβ Plaques in Cerebral Amyloid Angiopathy," *Bioconjugate Chemistry*, vol. 27, no. 5, pp. 1314–1323, 2016.

[68] H. Watanabe, M. Ono, S. Iikuni et al., "A 68Ga complex based on benzofuran scaffold for the detection of β-amyloid plaques," *Bioorganic & Medicinal Chemistry Letters*, vol. 24, no. 20, pp. 4834–4837, 2014.

[69] D. Cressier, M. Dhilly, T. T. Cao Pham et al., "Gallium-68 Complexes Conjugated to Pittsburgh Compound B: Radiolabeling and Biological Evaluation," *Molecular Imaging and Biology*, vol. 18, no. 3, pp. 334–343, 2016.

[70] D. Satpati, C. Arjun, R. Krishnamohan, G. Samuel, and S. Banerjee, "68Ga-labeled Ciprofloxacin Conjugates as Radiotracers for Targeting Bacterial Infection," *Chemical Biology & Drug Design*, vol. 87, no. 5, pp. 680–686, 2016.

[71] T. Ebenhan, N. Chadwick, and M. M. Sathekge, "Peptide synthesis, characterization and ^{68}Ga-radiolabeling of NOTA-conjugated ubiquicidin fragments for prospective infection imaging with PET/CT," *Nuclear Medicine and Biology*, vol. 41, no. 5, pp. 390–400, 2014.

[72] T. Ebenhan, J. R. Zeevaart, and J. D. Venter, "Preclinical evaluation of 68Ga-labeled 1, 4, 7-triazacyclononane-1, 4, 7-triacetic acid-ubiquicidin as a radioligand for PET infection imaging," *Journal of Nuclear Medicine*, vol. 55, no. 2, pp. 308–314, 2014.

[73] B. B. Mokaleng, T. Ebenhan, S. Ramesh et al., "Synthesis, ^{68}Ga-radiolabeling, and preliminary in vivo assessment of a depsipeptide-derived compound as a potential PET/CT infection imaging agent," *BioMed Research International*, vol. 2015, Article ID 284354, 2015.

[74] T. Ebenhan, B. Mokaleng, J. Venter, H. Kruger, J. Zeevaart, and M. Sathekge, "Preclinical Assessment of a 68Ga-DOTA-Functionalized Depsipeptide as a Radiodiagnostic Infection Imaging Agent," *Molecules*, vol. 22, no. 9, p. 1403, 2017.

[75] S. Chopra, B. Singh, A. Koul, A. Mishra, and H. Wester, "Synthesis of DOTA conjugated GF-17 and RAWVAWR-NH2 and radiolabeling with 68Ga as a potential PET tracer for infection imaging," *J Nucl Med*, vol. 57, Supplement 2, p. 1115, 2016.

[76] M. Petrik, H. Haas, P. Laverman et al., " ^{68}Ga-triacetylfusarinine C and ^{68}Ga-ferrioxamine e for aspergillus infection imaging: uptake specificity in various microorganisms," *Molecular Imaging and Biology*, vol. 16, no. 1, pp. 102–108, 2014.

[77] V. Kumar and D. K. Boddeti, " ^{68}Ga-radiopharmaceuticals for PET imaging of infection and inflammation," *Recent Results in Cancer Research*, vol. 194, pp. 189–219, 2013.

[78] M. Vorster, A. Maes, A. Jacobs et al., "Evaluating the possible role of 68Ga-citrate PET/CT in the characterization of indeterminate lung lesions," *Annals of Nuclear Medicine*, vol. 28, no. 6, pp. 523–530, 2014.

[79] M. Vorster, B. Mokaleng, M. M. Sathekge, and T. Ebenhan, "A modified technique for efficient radiolabeling of 68Ga-citrate from a SnO2-based 68Ge/68Ga generator for better infection imaging," *Hellenic Journal of Nuclear Medicine*, vol. 16, no. 3, pp. 193–198, 2013.

[80] S. Salomaeki, J. Kemppainen, U. Hohenthal et al., "Head-to-head comparison of 68Ga-Citrate and 18F-FDG PET/CT for detection of infectious foci in patients with staphylococcus aureus bacteraemia," *Contrast Media & Molecular Imaging*, vol. 2017, p. 8, 2017.

[81] L. Fass, "Imaging and cancer: a review," *Molecular Oncology*, vol. 2, no. 2, pp. 115–152, 2008.

[82] A. Chopra, L. Shan, W. C. Eckelman et al., "Molecular imaging and contrast agent database (MICAD): Evolution and progress," *Molecular Imaging and Biology*, vol. 14, no. 1, pp. 4–13, 2012.

[83] A. Sánchez-Crespo, P. Andreo, and S. A. Larsson, "Positron flight in human tissues and its influence on PET image spatial resolution," *European Journal of Nuclear Medicine and Molecular Imaging*, vol. 31, no. 1, pp. 44–51, 2004.

[84] H. W. A. M. De Jong, L. Perk, G. W. M. Visser, R. Boellaard, G. A. M. S. Van Dongen, and A. A. Lammertsma, "High resolution PET imaging characteristics of68Ga, 124i and89Zr compared to18F," in *Proceedings of the Nuclear Science Symposium Conference Record, 2005 IEEE*, pp. 1624–1627, Puerto Rico, October 2005.

[85] I. Velikyan, A. Sundin, B. Eriksson et al., "In vivo binding of [68Ga]-DOTATOC to somatostatin receptors in neuroendocrine tumours - impact of peptide mass," *Nuclear Medicine and Biology*, vol. 37, no. 3, pp. 265–275, 2010.

[86] U. Eberlein and M. Lassmann, "Dosimetry of [68Ga]-labeled compounds," *Applied Radiation and Isotopes*, vol. 76, pp. 70–74, 2013.

[87] C. Pettinato, A. Sarnelli, M. Di Donna et al., "68Ga-DOTANOC: Biodistribution and dosimetry in patients affected by neuroendocrine tumors," *European Journal of Nuclear Medicine and Molecular Imaging*, vol. 35, no. 1, pp. 72–79, 2008.

[88] B. P. Burke, G. S. Clemente, and S. J. Archibald, "Recent advances in chelator design and labelling methodology for 68Ga radiopharmaceuticals," *Journal of Labelled Compounds and Radiopharmaceuticals*, vol. 57, no. 4, pp. 239–243, 2014.

[89] I. Velikyan, U. Rosenström, S. Estrada et al., "Synthesis and preclinical evaluation of 68Ga-labeled collagelin analogs for imaging and quantification of fibrosis," *Nuclear Medicine and Biology*, vol. 41, no. 9, pp. 728–736, 2014.

[90] M. F. Ferreira, G. Pereira, J. P. André, and etal C., "Ga[NO2A-N-(α-amino)propionate] chelates: Synthesis and evaluation as potential tracers for 68Ga PET," *Dalton Transactions*, vol. 43, no. 21, pp. 8037–8047, 2014.

[91] J. Notni, J. Šimeček, and H.-J. Wester, "Phosphinic acid functionalized polyazacycloalkane chelators for radiodiagnostics and radiotherapeutics: Unique characteristics and applications," *ChemMedChem*, vol. 9, no. 6, pp. 1107–1115, 2014.

[92] J. Simeček, O. Zemek, P. Hermann, J. Notni, and H. J. Wester, "Tailored gallium(III) chelator NOPO: synthesis, characterization, bioconjugation, and application in preclinical Ga-68-PET imaging," *Molecular Pharmaceutics*, 2013.

[93] D. Parker, B. P. Waldron, and D. S. Yufit, "Crystallographic and solution NMR structural analyses of four hexacoordinated gallium(iii) complexes based on ligands derived from 6-amino-perhydro-1,4-diazepine," *Dalton Transactions*, vol. 42, no. 22, pp. 8001–8008, 2013.

[94] B. P. Waldron, D. Parker, C. Burchardt, D. S. Yufit, M. Zimny, and F. Roesch, "Structure and stability of hexadentate complexes of ligands based on AAZTA for efficient PET labelling with gallium-68," *Chemical Communications*, vol. 49, no. 6, pp. 579–581, 2013.

[95] D. Parker and B. P. Waldron, "Conformational analysis and synthetic approaches to polydentate perhydro-diazepine ligands for the complexation of gallium(iii)," *Organic & Biomolecular Chemistry*, vol. 11, no. 17, pp. 2827–2838, 2013.

[96] I. Velikyan, H. Maecke, and B. Langstrom, "Convenient preparation of 68Ga-based PET-radiopharmaceuticals at room temperature," *Bioconjugate Chemistry*, vol. 19, no. 2, pp. 569–573, 2008.

[97] J. Erchegyi, R. Cescato, B. Waser, J. E. Rivier, and J. C. Reubi, "N-Imidazolebenzyl-histidine substitution in somatostatin and in its octapeptide analogue modulates receptor selectivity and function," *Journal of Medicinal Chemistry*, vol. 54, no. 17, pp. 5981–5987, 2011.

[98] R. Saha, N. Saha, R. S. Donofrio, and L. L. Bestervelt, "Microbial siderophores: A mini review," *Journal of Basic Microbiology*, vol. 53, no. 4, pp. 303–317, 2013.

[99] V. Nikolova, S. Angelova, N. Markova, and T. Dudev, "Gallium as a Therapeutic Agent: A Thermodynamic Evaluation of the Competition between Ga3+ and Fe3+ Ions in Metalloproteins," *The Journal of Physical Chemistry B*, vol. 120, no. 9, pp. 2241–2248, 2016.

[100] C. R. Chitambar, "Gallium and its competing roles with iron in biological systems," *Biochimica et Biophysica Acta (BBA) - Molecular Cell Research*, vol. 1863, no. 8, pp. 2044–2053, 2016.

[101] J. A. Lessa, M. A. Soares, and R. G. dos Santos, "Gallium(III) complexes with 2-acetylpyridine-derived thiosemicarbazones: antimicrobial and cytotoxic effects and investigation on the interactions with tubulin," *BioMetals*, vol. 26, pp. 151–165, 2013.

[102] M. van Oosten, M. Hahn, L. M. A. Crane et al., "Targeted imaging of bacterial infections: Advances, hurdles and hopes," *FEMS Microbiology Reviews*, vol. 39, no. 6, pp. 892–916, 2015.

[103] M. Vorster, A. Maes, C. V. D. Wiele, and M. Sathekge, "Gallium-68 PET: A Powerful Generator-based Alternative to Infection and Inflammation Imaging," *Seminars in Nuclear Medicine*, vol. 46, no. 5, pp. 436–447, 2016.

[104] M. Kircher and C. Lapa, "Novel Noninvasive Nuclear Medicine Imaging Techniques for Cardiac Inflammation," *Current Cardiovascular Imaging Reports*, vol. 10, no. 2, article no. 6, 2017.

[105] D. A. Hammoud, "Molecular imaging of inflammation: Current status," *Journal of Nuclear Medicine*, vol. 57, no. 8, pp. 1161–1165, 2016.

[106] D. R. Brenner, D. Scherer, K. Muir et al., "A review of the application of inflammatory biomarkers in epidemiologic cancer research," *Cancer Epidemiology, Biomarkers & Prevention*, vol. 23, no. 9, pp. 1729–1751, 2014.

[107] M. D. Turner, B. Nedjai, T. Hurst, and D. J. Pennington, "Cytokines and chemokines: at the crossroads of cell signalling and inflammatory disease," *Biochimica et Biophysica Acta (BBA) - Molecular Cell Research*, vol. 1843, no. 11, pp. 2563–2582, 2014.

[108] L. Werner, H. Guzner-Gur, and I. Dotan, "Involvement of CXCR4/CXCR7/CXCL12 interactions in inflammatory bowel disease," *Theranostics*, vol. 3, no. 1, pp. 40–46, 2013.

[109] S. Jalkanen and M. Salmi, "VAP-1 and CD73, endothelial cell surface enzymes in leukocyte extravasation," *Arteriosclerosis, Thrombosis, and Vascular Biology*, vol. 28, no. 1, pp. 18–26, 2008.

[110] G. Malviya, F. Galli, I. Sonni, and A. Signore, "Imaging T-lymphocytes in inflammatory diseases: A nuclear medicine approach," *The Quarterly Journal of Nuclear Medicine and Molecular Imaging*, vol. 58, no. 3, pp. 237–257, 2014.

[111] S. Gratz, H. J. Rennen, O. C. Boerman, W. J. Oyen, and P. Burma, "(99 m)Tc-interleukin-8 for imaging acute osteomyelitis," *Journal of Nuclear Medicine*, vol. 42, no. 8, pp. 1257–1264, 2001.

[112] S. Gratz, H. J. Rennen, O. C. Boerman, W. J. Oyen, and F. H. Corstens, "Rapid imaging of experimental colitis with (99 m)Tc-interleukin-8 in rabbits," *Journal of Nuclear Medicne*, vol. 42, no. 6, pp. 917–923, 2001.

[113] C. Alkim, H. Alkim, A. R. Koksal, S. Boga, and I. Sen, "Angiogenesis in inflammatory bowel disease," *International Journal of Inflammation*, vol. 2015, Article ID 970890, 2015.

[114] I. S. Alam, T. H. Witney, G. Tomasi et al., "Radiolabeled RGD tracer kinetics annotates differential $\alpha v\beta 3$ integrin expression linked to cell intrinsic and vessel expression," *Molecular Imaging and Biology*, vol. 16, no. 4, pp. 558–566, 2014.

[115] J. Notni, K. Pohle, and H.-J. Wester, "Be spoilt for choice with radiolabelled RGD peptides: Preclinical evaluation of 68Ga-TRAP(RGD)3," *Nuclear Medicine and Biology*, vol. 40, no. 1, pp. 33–41, 2013.

[116] J. Oxboel, M. Brandt-Larsen, C. Schjoeth-Eskesen et al., "Comparison of two new angiogenesis PET tracers 68Ga-NODAGA-E[c(RGDyK)]2 and 64Cu-NODAGA-E[c(RGDyK)]2; in vivo imaging studies in human xenograft tumors," *Nuclear Medicine and Biology*, vol. 41, no. 3, pp. 259–267, 2014.

[117] J. Šimeček, J. Notni, T. G. Kapp, H. Kessler, and H.-J. Wester, "Benefits of NOPO as chelator in gallium-68 peptides, exemplified by preclinical characterization of 68Ga-NOPO-c(RGDfK)," *Molecular Pharmaceutics*, vol. 11, no. 5, pp. 1687–1695, 2014.

[118] M. Trajkovic-Arsic, P. Mohajerani, A. Sarantopoulos et al., "Multimodal molecular imaging of integrin avb3 for in vivo detection of pancreatic cancer," *Journal of Nuclear Medicine*, vol. 55, no. 3, pp. 446–451, 2014.

[119] H. Cai and P. S. Conti, "RGD-based PET tracers for imaging receptor integrin α v$\beta 3$ expression," *Journal of Labelled Compounds and Radiopharmaceuticals*, vol. 56, no. 5, pp. 264–279, 2013.

[120] I. Dijkgraaf, S. Y. A. Terry, W. J. Mcbride et al., "Imaging integrin alpha-v-beta-3 expression in tumors with an 18F-labeled dimeric RGD peptide," *Contrast Media & Molecular Imaging*, vol. 8, no. 3, pp. 238–245, 2013.

[121] P. A. Knetsch, M. Petrik, C. Rangger et al., "[68Ga]NS3-RGD and [68Ga] Oxo-DO3A-RGD for imaging $\alpha v\beta 3$ integrin expression: Synthesis, evaluation, and comparison," *Nuclear Medicine and Biology*, vol. 40, no. 1, pp. 65–72, 2013.

[122] Z. Liu and F. Wang, "Development of RGD-based radiotracers for tumor imaging and therapy: Translating from bench to bedside," *Current Molecular Medicine*, vol. 13, no. 10, pp. 1487–1505, 2013.

[123] H. Choi, J. H. Phi, J. C. Paeng et al., "Imaging of integrin $\alpha v\beta 3$ expression using 68Ga-RGD positron emission tomography in pediatric cerebral infarct," *Molecular Imaging*, vol. 12, no. 4, pp. 213–217, 2013.

[124] H.-J. Yoon, K. W. Kang, I. K. Chun et al., "Correlation of breast cancer subtypes, based on estrogen receptor, progesterone receptor, and HER2, with functional imaging parameters from 68Ga-RGD PET/CT and 18F-FDG PET/CT," *European Journal of Nuclear Medicine and Molecular Imaging*, vol. 41, no. 8, pp. 1534–1543, 2014.

[125] R. P. Baum, H. R. Kulkarni, D. Müller et al., "First-in-human study demonstrating tumor-angiogenesis by PET/CT imaging with ^{68}Ga-NODAGA-THERANOST, a high-affinity peptidomimetic for $\alpha v\beta 3$ integrin receptor targeting," *Cancer Biotherapy and Radiopharmaceuticals*, vol. 30, no. 4, pp. 152–159, 2015.

[126] R. Haubner, A. Finkenstedt, A. Stegmayr et al., "[68Ga]NODAGA-RGD – Metabolic stability, biodistribution, and dosimetry data from patients with hepatocellular carcinoma and liver cirrhosis," *European Journal of Nuclear Medicine and Molecular Imaging*, vol. 43, no. 11, pp. 2005–2013, 2016.

[127] V. López-Rodríguez, C. Galindo-Sarco, F. O. García-Pérez, G. Ferro-Flores, O. Arrieta, and M. A. Ávila-Rodríguez, "PET-based human dosimetry of the dimeric $\alpha v\beta 3$ integrin ligand 68Ga-DOTA-E-[c(RGDfK)]2, a potential tracer for imaging tumor angiogenesis," *Journal of Nuclear Medicine*, vol. 57, no. 3, pp. 404–409, 2016.

[128] M. V. Backer, Z. Levashova, V. Patel et al., "Molecular imaging of VEGF receptors in angiogenic vasculature with single-chain VEGF-based probes," *Nature Medicine*, vol. 13, no. 4, pp. 504–509, 2007.

[129] M. V. Backer, Z. Levashova, R. Levenson, F. G. Blankenberg, and J. M. Backer, "Cysteine-containing fusion tag for site-specific conjugation of therapeutic and imaging agents to targeting proteins," *Methods in Molecular Biology (Clifton, N.J.)*, vol. 494, pp. 275–294, 2008.

[130] M. Eder, A. V. Krivoshein, M. Backer, J. M. Backer, U. Haberkorn, and M. Eisenhut, "ScVEGF-PEG-HBED-CC and scVEGF-PEG-NOTA conjugates: comparison of easy-to-label recombinant proteins for [68Ga]PET imaging of VEGF receptors in angiogenic vasculature," *Nuclear Medicine and Biology*, vol. 37, no. 4, pp. 405–412, 2010.

[131] E. Blom, I. Velikyan, A. Monazzam, P. Razifar et al., "Synthesis and characterization of scVEGF-PEG-[68Ga]NOTA and scVEGF-PEG-[68Ga]DOTA PET tracers," *Journal of Labelled*

Compounds and Radiopharmaceuticals, vol. 54, no. 11, pp. 685–692, 2011.

[132] S. Gratz, M. Béhé, and O. C. Boerman, "^{99m}Tc-E-selectin binding peptide for imaging acute osteomyelitis in a novel rat model," *Nuclear Medicine Communications*, vol. 22, no. 9, pp. 1003–1013, 2001.

[133] S. B. Jensen, M. Käkelä, L. Jødal et al., "Exploring the radiosynthesis and in vitro characteristics of [68Ga]Ga-DOTA-Siglec-9," *Journal of Labelled Compounds and Radiopharmaceuticals*, vol. 60, no. 9, pp. 439–449, 2017.

[134] B. A. Teicher and S. P. Fricker, "CXCL12 (SDF-1)/CXCR4 pathway in cancer," *Clinical Cancer Research*, vol. 16, no. 11, pp. 2927–2931, 2010.

[135] O. Jacobson, I. D. Weiss, D. O. Kiesewetter, J. M. Farber, and X. Chen, "PET of tumor CXCR4 expression with 4-18F-T140," *Journal of Nuclear Medicine*, vol. 51, no. 11, pp. 1796–1804, 2010.

[136] A. Aghanejad, A. R. Jalilian, Y. Fazaeli et al., "Synthesis and evaluation of [67Ga]-AMD3100: A novel imaging agent for targeting the chemokine receptor CXCR4," *Scientia Pharmaceutica*, vol. 82, no. 1, pp. 29–42, 2014.

[137] O. Jacobson, I. D. Weiss, L. P. Szajek et al., "PET imaging of CXCR4 using copper-64 labeled peptide antagonist," *Theranostics*, vol. 1, pp. 251–262, 2011.

[138] O. Jacobson, I. D. Weiss, L. P. Szajek et al., "Improvement of CXCR4 tracer specificity for PET imaging," *Journal of Controlled Release*, vol. 157, no. 2, pp. 216–223, 2012.

[139] H. J. Wester, U. Keller, M. Schottelius et al., "Disclosing the CXCR4 expression in lymphoproliferative diseases by targeted molecular imaging," *Theranostics*, vol. 5, no. 6, pp. 618–630, 2015.

[140] E. Gourni, O. Demmer, M. Schottelius et al., "PET of CXCR4 expression by a 68Ga-labeled highly specific targeted contrast agent," *Journal of Nuclear Medicine*, vol. 52, no. 11, pp. 1803–1810, 2011.

[141] O. Demmer, I. Dijkgraaf, U. Schumacher et al., "Design, synthesis, and functionalization of dimeric peptides targeting chemokine receptor CXCR4," *Journal of Medicinal Chemistry*, vol. 54, no. 21, pp. 7648–7662, 2011.

[142] O. Demmer, E. Gourni, U. Schumacher, H. Kessler, and H.-J. Wester, "PET Imaging of CXCR4 Receptors in Cancer by a New Optimized Ligand," *ChemMedChem*, vol. 6, no. 10, pp. 1789–1791, 2011.

[143] U. Hennrich, L. Seyler, M. Schäfer et al., "Synthesis and in vitro evaluation of 68Ga-DOTA-4-FBn-TN14003, a novel tracer for the imaging of CXCR4 expression," *Bioorganic & Medicinal Chemistry*, vol. 20, no. 4, pp. 1502–1510, 2012.

[144] G. P. C. George, E. Stevens, O. Åberg et al., "Preclinical evaluation of a CXCR4-specific 68Ga-labelled TN14003 derivative for cancer PET imaging," *Bioorganic & Medicinal Chemistry*, vol. 22, no. 2, pp. 796–803, 2014.

[145] S. Poty, E. Gourni, P. Désogère et al., "AMD3100: A Versatile Platform for CXCR4 Targeting 68Ga-Based Radiopharmaceuticals," *Bioconjugate Chemistry*, vol. 27, no. 3, pp. 752–761, 2016.

[146] K. Philipp-Abbrederis, K. Herrmann, S. Knop et al., "In vivo molecular imaging of chemokine receptor CXCR4 expression in patients with advanced multiple myeloma," *EMBO Molecular Medicine*, vol. 7, no. 4, pp. 477–487, 2015.

[147] Z. Wang, M. Zhang, L. Wang et al., "Prospective study of 68Ga-NOTA-NFB: Radiation dosimetry in healthy volunteers and first application in glioma patients," *Theranostics*, vol. 5, no. 8, pp. 882–889, 2015.

[148] I. M. Jackson, P. J. Scott, and S. Thompson, "Clinical Applications of Radiolabeled Peptides for PET," *Seminars in Nuclear Medicine*, vol. 47, no. 5, pp. 493–523, 2017.

[149] C. Lapa, T. Reiter, R. A. Werner et al., "[68Ga]Pentixafor-PET/CT for Imaging of Chemokine Receptor 4 Expression after Myocardial Infarction," *JACC: Cardiovascular Imaging*, vol. 8, no. 12, pp. 1466–1468, 2015.

[150] C. Rischpler, S. G. Nekolla, H. Kossmann et al., "Upregulated myocardial CXCR4-expression after myocardial infarction assessed by simultaneous GA-68 pentixafor PET/MRI," *Journal of Nuclear Cardiology*, vol. 23, no. 1, pp. 131–133, 2016.

[151] F. Hyafil, J. Pelisek, I. Laitinen et al., "Imaging the Cytokine Receptor CXCR4 in atherosclerotic plaques with the radiotracer 68Ga-Pentixafor for PET," *Journal of Nuclear Medicine*, vol. 58, no. 3, pp. 499–506, 2017.

[152] Y. Yi, "Folate receptor-targeted diagnostics and therapeutics for inflammatory diseases," *Immune Network*, vol. 16, no. 6, pp. 337–343, 2016.

[153] C. M. Paulos, M. J. Turk, G. J. Breur, and P. S. Low, "Folate receptor-mediated targeting of therapeutic and imaging agents to activated macrophages in rheumatoid arthritis," *Advanced Drug Delivery Reviews*, vol. 56, no. 8, pp. 1205–1217, 2004.

[154] W. Han, R. Zaynagetdinov, F. E. Yull et al., "Molecular imaging of folate receptor β-positive macrophages during acute lung inflammation," *American Journal of Respiratory Cell and Molecular Biology*, vol. 53, no. 1, pp. 50–59, 2015.

[155] B. Kühle, C. Müller, and T. L. Ross, "A Novel 68Ga-Labeled pteroic acid-based PET tracer for tumor imaging via the folate receptor," *Recent Results in Cancer Research*, vol. 194, pp. 257–267, 2013.

[156] C. Brand, V. A. Longo, M. Groaning, W. A. Weber, and T. Reiner, "Development of a New Folate-Derived Ga-68-Based PET Imaging Agent," *Molecular Imaging and Biology*, vol. 19, no. 5, pp. 754–761, 2017.

[157] M. Fani, X. Wang, G. Nicolas et al., "Development of new folate-based PET radiotracers: Preclinical evaluation of 68Ga-DOTA-folate conjugates," *European Journal of Nuclear Medicine and Molecular Imaging*, vol. 38, no. 1, pp. 108–119, 2011.

[158] C. J. Mathias, M. R. Lewis, D. E. Reichert et al., "Preparation of 66Ga- and 68Ga-labeled Ga(III)-deferoxamine-folate as potential folate-receptor-targeted PET radiopharmaceuticals," *Nuclear Medicine and Biology*, vol. 30, no. 7, pp. 725–731, 2003.

[159] S.-M. Kim, N. Choi, S. Hwang et al., "Folate receptor-specific positron emission tomography imaging with folic acid-conjugated tissue inhibitor of metalloproteinase-2," *Bulletin of the Korean Chemical Society*, vol. 34, no. 11, pp. 3243–3248, 2013.

[160] M. Fani, M.-L. Tamma, G. P. Nicolas et al., "In vivo imaging of folate receptor positive tumor xenografts using novel 68Ga-NODAGA-folate conjugates," *Molecular Pharmaceutics*, vol. 9, no. 5, pp. 1136–1145, 2012.

[161] C. Müller and R. Schibli, "Prospects in folate receptor-targeted radionuclide therapy," *Frontiers in Oncology*, vol. 3, Article ID Article 249, 2013.

[162] A. Jain, A. Mathur, U. Pandey et al., "Synthesis and evaluation of a 68Ga labeled folic acid derivative for targeting folate receptors," *Applied Radiation and Isotopes*, vol. 116, pp. 77–84, 2016.

[163] W. Xia, A. R. Hilgenbrink, E. L. Matteson, M. B. Lockwood, J.-X. Cheng, and P. S. Low, "A functional folate receptor is induced during macrophage activation and can be used to target drugs to activated macrophages," *Blood*, vol. 113, no. 2, pp. 438–446, 2009.

[164] E. P. Krenning, W. A. P. Breeman, P. P. M. Kooij et al., "Localisation of endocrine-related tumours with radioiodinated analogue of somatostatin," *The Lancet*, vol. 1, no. 8632, pp. 242–244, 1989.

[165] E. P. Krenning, D. J. Kwekkeboom, W. H. Bakker et al., "Somatostatin receptor scintigraphy with [^{111}In-DTPA-d-Phe^{1}]- and [^{123}I-Tyr^{3}]-octreotide: the Rotterdam experience with more than 1000 patients," *European Journal of Nuclear Medicine and Molecular Imaging*, vol. 20, no. 8, pp. 716–731, 1993.

[166] A. Stahl, G. Meisetschläger, M. Schottelius et al., "[123I]MtrTOCA, a radioiodinated and carbohydrated analogue of octreotide: Scintigraphic comparison with [111In]octreotide," *European Journal of Nuclear Medicine and Molecular Imaging*, vol. 33, no. 1, pp. 45–52, 2006.

[167] R. Lebtahi, J. le Cloirec, C. Houzard et al., "Detection of neuroendocrine tumors: 99mTc-P829 scintigraphy compared with 111In-pentetreotide scintigraphy," *Journal of Nuclear Medicine*, vol. 43, no. 7, pp. 889–895, 2002.

[168] C. Decristoforo, T. Maina, B. Nock, M. Gabriel, P. Cordopatis, and R. Moncayo, "99mTc-demotate 1: First data in tumour patients - Results of a pilot/phase I study," *European Journal of Nuclear Medicine and Molecular Imaging*, vol. 30, no. 9, pp. 1211–1219, 2003.

[169] C. Decristoforo, S. J. Mather, W. Cholewinski, E. Donnemiller, G. Riccabona, and R. Moncayo, "(99m)Tc-EDDA/HYNIC-TOC: A new (99m)Tc-labelled radiopharmaceutical for imaging somatostatin receptor-positive tumours: First clinical results and intra-patient comparison with 111In-labelled octreotide derivatives," *European Journal of Nuclear Medicine and Molecular Imaging*, vol. 27, no. 9, pp. 1318–1325, 2000.

[170] A. Hubalewska-Dydejczyk, K. Fröss-Baron, R. Mikołajczak et al., "99mTc-EDDA/HYNIC-octreotate scintigraphy, an efficient method for the detection and staging of carcinoid tumours: Results of 3 years' experience," *European Journal of Nuclear Medicine and Molecular Imaging*, vol. 33, no. 10, pp. 1123–1133, 2006.

[171] M. Bangard, M. Béhé, S. Guhlke et al., "Detection of somatostatin receptor-positive tumours using the new 99mC-tricine-HYNIC-D-Phe1-Tyr3-octreotide: First results in patients and comparison with 111In-DTPA-D-Phe1-octreotide," *European Journal of Nuclear Medicine and Molecular Imaging*, vol. 27, no. 6, pp. 628–637, 2000.

[172] A. Helisch, G. J. Fórster, H. Reber et al., "Pre-therapeutic dosimetry and biodistribution of 86Y-DOTA- Phe1-Tyr3-octreotide versus 111In-pentetreotide in patients with advanced neuroendocrine tumours," *European Journal of Nuclear Medicine and Molecular Imaging*, vol. 31, no. 10, pp. 1386–1392, 2004.

[173] M. Henze, J. Schuhmacher, P. Hipp et al., "PET imaging of somatostatin receptors using [68GA]DOTA-D-Phe1-Tyr3-Octreotide: First results in patients with meningiomas," *Journal of Nuclear Medicine*, vol. 42, no. 7, pp. 1053–1056, 2001.

[174] I. Kayani, J. B. Bomanji, A. Groves et al., "Functional imaging of neuroendocrine tumors with combined PET/CT using 68Ga-DOTATATE (Dota-DPhe1, Tyr3-octreotate) and 18F-FDG," *Cancer*, vol. 112, no. 11, pp. 2447–2455, 2008.

[175] A. Al-Nahhas, "Nuclear medicine imaging of neuroendocrine tumours," *Clinical Medicine*, vol. 12, no. 4, pp. 377–380, 2012.

[176] V. Ambrosini, S. Nicolini, P. Caroli et al., "PET/CT imaging in different types of lung cancer: an overview," *European Journal of Radiology*, vol. 81, no. 5, pp. 988–1001, 2012.

[177] V. Ambrosini, D. Campana, P. Tomassetti, and S. Fanti, "68Ga-labelled peptides for diagnosis of gastroenteropancreatic NET," *European Journal of Nuclear Medicine and Molecular Imaging*, vol. 39, no. 1, pp. S52–S60, 2012.

[178] K. E. Oberg, J.-C. Reubi, D. J. Kwekkeboom, and E. P. Krenning, "Role of somatostatins in gastroenteropancreatic neuroendocrine tumor development and therapy," *Gastroenterology*, vol. 139, no. 3, pp. 753-753, 2010.

[179] K. Öberg, "Gallium-68 somatostatin receptor PET/CT: Is it time to replace 111Indium DTPA octreotide for patients with neuroendocrine tumors?" *Endocrine Journal*, vol. 42, no. 1, pp. 3-4, 2012.

[180] R. Srirajaskanthan, I. Kayani, A. M. Quigley, J. Soh, M. E. Caplin, and J. Bomanji, "The role of 68Ga-DOTATATE PET in patients with neuroendocrine tumors and negative or equivocal findings on 111In-DTPA-octreotide scintigraphy," *Journal of Nuclear Medicine*, vol. 51, no. 6, pp. 875–882, 2010.

[181] A. Kroiss, D. Putzer, and C. Uprimny, "Functional imaging in phaeochromocytoma and neuroblastoma with 68Ga-DOTA-Tyr3-octreotide positron emission tomography and 123I-metaiodobenzylguanidine," *European Journal of Nuclear Medicine and Molecular Imaging*, vol. 38, no. 5, pp. 865–873, 2011.

[182] M. Naji, C. Zhao, S. J. Welsh et al., "68Ga-DOTA-TATE PET vs. 123I-MIBG in identifying malignant neural crest tumours," *Molecular Imaging and Biology*, vol. 13, no. 4, pp. 769–775, 2011.

[183] V. Ambrosini, P. Tomassetti, P. Castellucci et al., "Comparison between 68Ga-DOTA-NOC and 18F-DOPA PET for the detection of gastro-entero-pancreatic and lung neuro-endocrine tumours," *European Journal of Nuclear Medicine and Molecular Imaging*, vol. 35, no. 8, pp. 1431–1438, 2008.

[184] D. Putzer, M. Gabriel, B. Henninger et al., "Bone metastases in patients with neuroendocrine tumor: 68Ga- DOTA-Tyr3-octreotide PET in comparison to CT and bone scintigraphy," *Journal of Nuclear Medicine*, vol. 50, no. 8, pp. 1214–1221, 2009.

[185] L. K. Anzola-Fuentes, M. Chianelli, F. Galli et al., "Somatostatin receptor scintigraphy in patients with rheumatoid arthritis and secondary Sjögren's syndrome treated with Infliximab: a pilot study," *EJNMMI Research*, vol. 6, no. 1, article no. 49, 2016.

[186] T. Nobashi, Y. Nakamoto, T. Kubo et al., "The utility of PET/CT with 68Ga-DOTATOC in sarcoidosis: comparison with 67Ga-scintigraphy," *Annals of Nuclear Medicine*, vol. 30, no. 8, pp. 544–552, 2016.

[187] C. Boy, T. A. Heusner, T. D. Poeppel et al., "68Ga-DOTATOC PET/CT and somatostatin receptor (sst1-sst5) expression in normal human tissue: Correlation of sst2 mRNA and SUV max," *European Journal of Nuclear Medicine and Molecular Imaging*, vol. 38, no. 7, pp. 1224–1236, 2011.

[188] P. Rinne, S. Hellberg, M. Kiugel et al., "Comparison of Somatostatin Receptor 2-Targeting PET Tracers in the Detection of Mouse Atherosclerotic Plaques," *Molecular Imaging and Biology*, vol. 18, no. 1, pp. 99–108, 2016.

[189] M. Asti, E. Ferrari, S. Croci et al., "Synthesis and characterization of 68Ga-labeled curcumin and curcuminoid complexes as potential radiotracers for imaging of cancer and alzheimers disease," *Inorganic Chemistry*, vol. 53, no. 10, pp. 4922–4933, 2014.

[190] A. Signore, I. Santino, and A. W. J. M. Glaudemans, "In vivo imaging of microorganisms," *Clinical and Translational Imaging*, vol. 4, no. 3, pp. 161-162, 2016.

[191] S. Auletta, F. Galli, C. Lauri, D. Martinelli, I. Santino, and A. Signore, "Imaging bacteria with radiolabelled quinolones,

cephalosporins and siderophores for imaging infection: a systematic review," *Clinical and Translational Imaging*, vol. 4, no. 4, pp. 229–252, 2016.

[192] X. Ning, S. Lee, Z. Wang et al., "Maltodextrin-based imaging probes detect bacteria in vivo with high sensitivity and specificity," *Nature Materials*, vol. 10, no. 8, pp. 602–607, 2011.

[193] J. Ady and Y. Fong, "Imaging for infection: From visualization of inflammation to visualization of microbes," *Surgical Infections*, vol. 15, no. 6, pp. 700–707, 2014.

[194] J. M. Sierra, D. Rodriguez-Puig, A. Soriano, J. Mensa, C. Piera, and J. Vila, "Accumulation of 99mTc-ciprofloxacin in Staphylococcus aureus and Pseudomonas aeruginosa," *Antimicrobial Agents and Chemotherapy*, vol. 52, no. 7, pp. 2691-2692, 2008.

[195] D. I. Andersson and D. Hughes, "Microbiological effects of sublethal levels of antibiotics," *Nature Reviews Microbiology*, vol. 12, no. 7, pp. 465–478, 2014.

[196] N. Dumarey, D. Blocklet, T. Appelboom, L. Tant, and A. Schoutens, "Infecton is not specific for bacterial osteo-articular infective pathology," *European Journal of Nuclear Medicine and Molecular Imaging*, vol. 29, no. 4, pp. 530–535, 2002.

[197] K. E. Britton, D. W. Wareham, S. S. Das et al., "Imaging bacterial infection with 99mTc-ciprofloxacin (Infecton)," *Journal of Clinical Pathology*, vol. 55, no. 11, pp. 817–823, 2002.

[198] G. Ferro-Flores, M. A. Avila-Rodríguez, and F. O. García-Pérez, "Imaging of bacteria with radiolabeled ubiquicidin by SPECT and PET techniques," *Clinical and Translational Imaging*, vol. 4, no. 3, pp. 175–182, 2016.

[199] P. S. Hiemstra, M. T. van den Barselaar, M. Roest, P. H. Nibbering, and R. van Furth, "Ubiquicidin, a novel murine microbicidal protein present in the cytosolic fraction of macrophages," *Journal of Leukocyte Biology*, vol. 66, no. 3, pp. 423–428, 1999.

[200] M. S. Akhtar, A. Qaisar, J. Irfanullah et al., "Antimicrobial peptide 99mTc-ubiquicidin 29–41 as human infection-imaging agent: clinical trial," *Journal of Nuclear Medicne*, vol. 46, no. 4, pp. 567–573, 2005.

[201] M. Assadi, K. Vahdat, I. Nabipour et al., "Diagnostic value of 99mTc-ubiquicidin scintigraphy for osteomyelitis and comparisons with 99mTc-methylene diphosphonate scintigraphy and magnetic resonance imaging," *Nuclear Medicine Communications*, vol. 32, no. 8, pp. 716–723, 2011.

[202] T. Emery, "Exchange of Iron by Gallium in Siderophores," *Biochemistry*, vol. 25, no. 16, pp. 4629–4633, 1986.

[203] M. Petrik, C. Zhai, H. Haas, and C. Decristoforo, "Siderophores for molecular imaging applications," *Clinical and Translational Imaging*, vol. 5, no. 1, pp. 15–27, 2017.

[204] H. J. Flint, E. A. Bayer, M. T. Rincon, R. Lamed, and B. A. White, "Polysaccharide utilization by gut bacteria: potential for new insights from genomic analysis," *Nature Reviews Microbiology*, vol. 6, no. 2, pp. 121–131, 2008.

[205] G. Gowrishankar, M. Namavari, E. B. Jouannot et al., "Investigation of 6-[18F]-fluoromaltose as a novel PET tracer for imaging bacterial infection," *PLoS ONE*, vol. 9, no. 9, Article ID e107951, 2014.

[206] N. Gholipour, M. Akhlaghi, A. M. Kheirabadi et al., "Chelator-free radiolabeling of dextran with 68Ga for PET studies," *Journal of Radioanalytical and Nuclear Chemistry*, vol. 311, no. 3, pp. 1811–1817, 2017.

[207] C. Bettegowda, C. A. Foss, I. Cheong et al., "Imaging bacterial infections with radiolabeled 1-(2′-deoxy-2′- fluoro-β-D-arabinofuranosyl)-5-iodouracil," *Proceedings of the National Acadamy of Sciences of the United States of America*, vol. 102, no. 4, pp. 1145–1150, 2005.

[208] S. A. Soghomonyan, M. Doubrovin, J. Pike et al., "Positron emission tomography (PET) imaging of tumor-localized Salmonella expressing HSV1-TK," *Cancer Gene Therapy*, vol. 12, no. 1, pp. 101–108, 2005.

[209] C. Palestro, K. Nichols, S. Sheikh-Fayyaz, S. Dewey, P. Singhal, and K. Bhargava, "Can Gallium-68 PET differentiate acute interstitial nephritis from acute tubular necrosis?" *Journal of Nuclear Medicne*, vol. 57, Supplement 2, p. 551, 2016.

[210] A. J. Morguet, D. L. Munz, V. Ivančević et al., "Immunoscintigraphy using technetium-99m-labeled anti-NCA-95 antigranulocyte antibodies as an adjunct to echocardiography in subacute infective endocarditis," *Journal of the American College of Cardiology*, vol. 23, no. 5, pp. 1171–1178, 1994.

[211] C. van der Laken, O. Boerman, W. Oyen et al., "In Vivo Expression of Interleukin-1 Receptors during Various Experimentally Induced Inflammatory Conditions," *The Journal of Infectious Diseases*, vol. 177, no. 5, pp. 1398–1401, 1998.

[212] C. J. Van Der Laken, O. C. Boerman, W. J. G. Oyen, M. T. P. Van De Ven, J. W. M. Van Der Meer, and F. H. M. Corstens, "Scintigraphic detection of infection and inflammation: New developments with special emphasis on receptor interaction," *European Journal of Nuclear Medicine and Molecular Imaging*, vol. 25, no. 5, pp. 535–546, 1998.

[213] C. J. van der Laken, O. C. Boerman, W. J. G. Oyen, M. T. P. van de Ven, J. W. M. van der Meer, and F. H. M. Corstens, "Imaging of infection in rabbits with radioiodinated interleukin-1 (α and β), its receptor antagonist and a chemotactic peptide: a comparative study," *European Journal of Nuclear Medicine and Molecular Imaging*, vol. 25, no. 4, pp. 347–352, 1998.

[214] C. J. Van Der Laken, O. C. Boerman, W. J. G. Oyen, M. T. P. Van De Ven, F. H. M. Corstens, and J. W. M. Ven Der Meer, "The kinetics of radiolabelled interleukin-8 in infection and sterile inflammation," *Nuclear Medicine Communications*, vol. 19, no. 3, pp. 271–282, 1998.

[215] E. Lazzeri, P. Erba, M. Perri et al., "Scintigraphic imaging of vertebral osteomyelitis with 111in-biotin," *The Spine Journal*, vol. 33, no. 7, pp. E198–E204, 2008.

[216] E. Blom, B. Långström, and I. Velikyan, "68Ga-labeling of biotin analogues and their characterization," *Bioconjugate Chemistry*, vol. 20, no. 6, pp. 1146–1151, 2009.

[217] O. Eriksson, F. Carlsson, E. Blom et al., "Preclinical evaluation of a 68Ga-labeled biotin analogue for applications in islet transplantation," *Nuclear Medicine and Biology*, vol. 39, no. 3, pp. 415–421, 2012.

[218] E. A. Weinstein, A. A. Ordonez, V. P. DeMarco et al., "Imaging Enterobacteriaceae infection in vivo with ^{18}F-fluorodeoxysorbitol positron emission tomography," *Science Translational Medicine*, vol. 6, no. 259, p. 259ra146, 2014.

[219] K. M. Nielsen, M. H. Kyneb, A. K. O. Alstrup et al., "68Ga-labeled phage-display selected peptides as tracers for positron emission tomography imaging of Staphylococcus aureus biofilm-associated infections: Selection, radiolabelling and preliminary biological evaluation," *Nuclear Medicine and Biology*, vol. 43, no. 10, pp. 593–605, 2016.

[220] T. J. Mäkinen, P. Lankinen, T. Pöyhönen, J. Jalava, H. T. Aro, and A. Roivainen, "Comparison of 18F-FDG and 68Ga PET imaging in the assessment of experimental osteomyelitis due to Staphylococcus aureus," *European Journal of Nuclear Medicine and Molecular Imaging*, vol. 32, no. 11, pp. 1259–1268, 2005.

[221] J. M. U. Silvola, I. Laitinen, H. J. Sipilä et al., "Uptake of ^{68}gallium in atherosclerotic plaques in LDLR$^{-/-}$ApoB$^{100/100}$mice," *EJNMMI Research*, vol. 1, no. 1, pp. 1–8, 2011.

[222] T. A. Wynn, "Cellular and molecular mechanisms of fibrosis," *The Journal of Pathology*, vol. 214, no. 2, pp. 199–210, 2008.

[223] T. Derlin, D. Jonigk, J. Bauersachs, and F. M. Bengel, "Molecular Imaging of Chemokine Receptor CXCR4 in Non–Small Cell Lung Cancer Using 68Ga-Pentixafor PET/CT: Comparison With 18F-FDG," *Clinical Nuclear Medicine*, 2016.

[224] I. Velikyan, U. Rosenström, T. N. Bulenga, O. Eriksson, and G. Antoni, "Feasibility of multiple examinations using68ga-labelled collagelin analogues: Organ distribution in rat for extrapolation to human organ and whole-body radiation dosimetry," *Pharmaceuticals*, vol. 9, no. 2, article no. 31, 2016.

[225] S. Jadhav, M. Käkelä, J. Mäkilä et al., "Synthesis and in Vivo PET Imaging of Hyaluronan Conjugates of Oligonucleotides," *Bioconjugate Chemistry*, vol. 27, no. 2, pp. 391–403, 2016.

[226] A. Autio, A. Saraste, N. Kudomi et al., "Assessment of blood flow with (68) Ga-DOTA PET in experimental inflammation: a validation study using (15) O-water," *American Journal of Nuclear Medicine and Molecular Imaging*, vol. 4, no. 6, pp. 571–579, 2014.

[227] G. Davies, A. Rolle, A. Maurer et al., "Towards translational immunoPET/MR imaging of invasive pulmonary aspergillosis: the Humanised Monoclonal Antibody JF5 detects in vivo," *Theranostics*, vol. 7, no. 14, pp. 3398–3414, 2017.

[228] D. Goodwin, C. Meares, G. David et al., "Monoclonal antibodies as reversible equilibrium carriers of radiopharmaceuticals," *International Journal of Radiation Applications and Instrumentation. Part B: Nuclear Medicine and Biology*, vol. 13, no. 4, pp. 383–391, 1986.

[229] D. A. Goodwin, C. F. Mears, M. McTigue, and G. S. David, "Monoclonal antibody hapten radiopharmaceutical delivery," *Nuclear Medicine Communications*, vol. 7, no. 8, pp. 569–580, 1986.

[230] S. E. Halpern and R. O. Dillman, "Problems associated with radioimmunodetection and possibilities for future solutions," *J Biol Response Mod*, vol. 6, no. 3, pp. 235–262, 1987.

[231] H. Hong, J. Sun, and W. Cai, "Radionuclide-based cancer imaging targeting the carcinoembryonic antigen," *Biomarker Insights*, vol. 3, pp. 435–451, 2008.

[232] G. J. Förster, E. B. Santos, P. M. Smith-Jones, P. Zanzonico, and S. M. Larson, "Pretargeted radioimmunotherapy with a single-chain antibody/streptavidin construct and radiolabeled DOTA-biotin: Strategies for reduction of the renal dose," *Journal of Nuclear Medicine*, vol. 47, no. 1, pp. 140–149, 2006.

[233] Z. Yao, M. Zhang, H. Kobayashi et al., "Improved targeting of radiolabeled streptavidin in tumors pretargeted with biotinylated monoclonal antibodies through an avidin chase," *Journal of Nuclear Medicine*, vol. 36, no. 5, pp. 837–841, 1995.

[234] C-H. Chang, R. M. Sharkey, E. A. Rossi et al., "Molecular Advances in Pretargeting Radioimunotherapy with Bispecific Antibodies 1 Supported in part by USPHS Grant R01-CA-84379 from the NIH and Department of Energy Grant DE-FG01-00NE22941 (both to R. M. S.).1," *Mol Cancer Ther*, vol. 1, no. 7, pp. 553–563, 2002.

[235] R. M. Sharkey, E. A. Rossi, W. J. McBride, C.-H. Chang, and D. M. Goldenberg, "Recombinant Bispecific Monoclonal Antibodies Prepared by the Dock-and-Lock Strategy for Pretargeted Radioimmunotherapy," *Seminars in Nuclear Medicine*, vol. 40, no. 3, pp. 190–203, 2010.

[236] R. M. Sharkey, E. A. Rossi, C.-H. Chang, and D. M. Goldenberg, "Improved cancer therapy and molecular imaging with multivalent, multispecific antibodies," *Cancer Biotherapy and Radiopharmaceuticals*, vol. 25, no. 1, pp. 1–12, 2010.

[237] D. M. Goldenberg, R. M. Sharkey, G. Paganelli, J. Barbet, and J. Chatal, "Antibody pretargeting advances cancer radioimmunodetection and radioimmunotherapy," *Journal of Clinical Oncology*, vol. 24, no. 5, pp. 823–834, 2006.

[238] O. C. Boerman, F. G. van Schaijk, W. J. G. Oyen, and F. H. M. Corstens, "Pretargeted radioimmunotherapy of cancer: progress step by step," *Journal of Nuclear Medicine*, vol. 44, no. 3, pp. 400–411, 2003.

[239] J. Schuhmacher, S. Kaul, G. Klivényi et al., "Immunoscintigraphy with positron emission tomography: Gallium-68 chelate imaging of breast cancer pretargeted with bispecific anti-MUC1/anti-Ga chelate antibodies," *Cancer Research*, vol. 61, no. 9, pp. 3712–3717, 2001.

[240] J. Schuhmacher, G. Klivényi, S. Kaul et al., "Pretargeting of human mammary carcinoma xenografts with bispecific anti-MUC1/anti-Ga chelate antibodies and immunoscintigraphy with PET," *Nuclear Medicine and Biology*, vol. 28, no. 7, pp. 821–828, 2001.

[241] C. Somasundaram, S. Matzku, J. Schuhmacher, and M. Zöller, "Development of a bispecific monoclonal antibody against a gallium-67 chelate and the human melanoma-associated antigen p97 for potential use in pretargeted immunoscintigraphy," *Cancer Immunology, Immunotherapy*, vol. 36, no. 5, pp. 337–345, 1993.

[242] E. A. Rossi, D. L. Rossi, R. Stein, D. M. Goldenberg, and C.-H. Chang, "A bispecific antibody-IFNα2b immunocytokine targeting CD20 and HLA-DR is highly toxic to human lymphoma and multiple myeloma cells," *Cancer Research*, vol. 70, no. 19, pp. 7600–7609, 2010.

[243] R. M. Sharkey, H. Karacay, S. Litwin et al., "Improved therapeutic results by pretargeted radioimmunotherapy of non-Hodgkin's lymphoma with a new recombinant, trivalent, anti-CD20, bispecific antibody," *Cancer Research*, vol. 68, no. 13, pp. 5282–5290, 2008.

[244] G. L. Griffiths, C.-H. Chang, W. J. McBride et al., "Reagents and methods for PET using bispecific antibody pretargeting and 68Ga-radiolabeled bivalent hapten-peptide-chelate conjugates," *Journal of Nuclear Medicine*, vol. 45, no. 1, pp. 30–39, 2004.

[245] J. Watine, M. Miédougé, and B. Friedberg, "Carcinoembryonic antigen as an independent prognostic factor of recurrence and survival in patients resected for colorectal liver metastases: A systematic review," *Diseases of the Colon & Rectum*, vol. 44, no. 12, pp. 1791–1799, 2001.

[246] M. J. Goldstein and E. P. Mitchell, "Carcinoembryonic antigen in the staging and follow-up of patients with colorectal cancer," *Cancer Investigation*, vol. 23, no. 4, pp. 338–351, 2005.

[247] D. V. Gold, D. M. Goldenberg, H. Karacay et al., "A novel bispecific, trivalent antibody construct for targeting pancreatic carcinoma," *Cancer Research*, vol. 68, no. 12, pp. 4819–4826, 2008.

[248] J. Schuhmacher, G. Klivényi, R. Matys et al., "Multistep tumor targeting in nude mice using bispecific antibodies and a gallium chelate suitable for immunoscintigraphy with positron emission tomography," *Cancer Research*, vol. 55, no. 1, pp. 115–123, 1995.

[249] G. Klivényi, J. Schuhmacher, E. Patzelt et al., "Gallium-68 chelate imaging of human colon carcinoma xenografts pretargeted with bispecific anti-CD44(V6)/anti-gallium chelate antibodies," *Journal of Nuclear Medicine*, vol. 39, no. 10, pp. 1769–1776, 1998.

[250] M. Zoller, J. Schuhmacher, J. Reed, W. Maier-Borst, and S. Matzku, "Establishment and characterization of monoclonal

antibodies against an octahedral gallium chelate suitable for immunoscintigraphy with PET," *Journal of Nuclear Medicine*, vol. 33, no. 7, pp. 1366–1372, 1992.

[251] R. M. Sharkey, T. M. Cardillo, E. A. Rossi et al., "Signal amplification in molecular imaging by pretargeting a multivalent, bispecific antibody," *Nature Medicine*, vol. 11, no. 11, pp. 1250–1255, 2005.

[252] D. M. Goldenberg and R. M. Sharkey, "Novel radiolabeled antibody conjugates," *Oncogene*, vol. 26, no. 25, pp. 3734–3744, 2007.

[253] D. M. Goldenberg, E. A. Rossi, R. M. Sharkey, W. J. McBride, and C.-H. Chang, "Multifunctional antibodies by the dock-and-lock method for improved cancer imaging and therapy by pretargeting," *Journal of Nuclear Medicine*, vol. 49, no. 1, pp. 158–163, 2008.

[254] R. Schoffelen, R. M. Sharkey, D. M. Goldenberg et al., "Pre-targeted immuno-positron emission tomography imaging of carcinoembryonic antigen-expressing tumors with a bispecific antibody and a68Ga- And18F-labeled hapten peptide in mice with human tumor xenografts," *Molecular Cancer Therapeutics*, vol. 9, no. 4, pp. 1019–1027, 2010.

[255] E. S. Bos, W. H. Kuijpers, M. Meesters-Winters et al., "In vitro evaluation of DNA-DNA hybridization as a two-step approach in radioimmunotherapy of cancer," *Cancer Research*, vol. 54, no. 13, pp. 3479–3486, 1994.

[256] G. Paganelli, M. Bartolomei, M. Ferrari et al., "Pre-Targeted Locoregional Radioimmunotherapy with," *Cancer biotherapy and radiopharmaceuticals*, vol. 16, no. 3, pp. 227–235, 2001.

[257] A. Forero, P. L. Weiden, J. M. Vose et al., "Phase 1 trial of a novel anti-CD20 fusion protein in pretargeted radioimmunotherapy for B-cell non-Hodgkin lymphoma," *Blood*, vol. 104, no. 1, pp. 227–236, 2004.

[258] D. M. Goldenberg, C.-H. Chang, E. A. Rossi, W. J. McBride, and R. M. Sharkey, "Pretargeted molecular imaging and radioimmunotherapy," *Theranostics*, vol. 2, no. 5, pp. 523–540, 2012.

[259] H. Karacay, R. M. Sharkey, W. J. McBride, E. A. Rossi, C.-H. Chang, and D. M. Goldenberg, "Optimization of hapten-peptide labeling for pretargeted immunoPET of bispecific antibody using generator-produced 68Ga," *Journal of Nuclear Medicine*, vol. 52, no. 4, pp. 555–559, 2011.

[260] J. R. Oh and B. C. Ahn, "False-positive uptake on radioiodine whole-body scintigraphy: physiologic and pathologic variants unrelated to thyroid cancer," *American Journal of Nuclear Medicine and Molecular Imaging*, vol. 2, no. 2, pp. 141–150, 2012.

[261] E. Frampas, C. Rousseau, C. Bodet-Milin, J. Barbet, J.-F. Chatal, and F. Kraeber-Bodéré, "Improvement of radioimmunotherapy using pretargeting," *Frontiers in Oncology*, vol. 3, Article ID 00159, 2013.

[262] C. S. McKay and M. G. Finn, "Click chemistry in complex mixtures: Bioorthogonal bioconjugation," *Chemistry & Biology*, vol. 21, no. 9, pp. 1075–1101, 2014.

[263] B. L. Oliveira, Z. Guo, and G. J. Bernardes, "Inverse electron demand Diels–Alder reactions in chemical biology," *Chemical Society Reviews*, vol. 46, no. 16, pp. 4895–4950, 2017.

[264] B. Nichols, Z. Qin, J. Yang, D. R. Vera, and N. K. Devaraj, "68Ga chelating bioorthogonal tetrazine polymers for the multistep labeling of cancer biomarkers," *Chemical Communications*, vol. 50, no. 40, pp. 5215–5217, 2014.

[265] R. Rossin, P. R. Verkerk, S. M. van den Bosch et al., "In vivo chemistry for pretargeted tumor imaging in live mice," *Angewandte Chemie International Edition*, vol. 49, no. 19, pp. 3375–3378, 2010.

[266] B. M. Zeglis, K. K. Sevak, T. Reiner et al., "A pretargeted PET imaging strategy based on bioorthogonal diels-alder click chemistry," *Journal of Nuclear Medicine*, vol. 54, no. 8, pp. 1389–1396, 2013.

[267] J. L. Houghton, R. Membreno, D. Abdel-Atti et al., "Establishment of the invivo efficacy of pretargeted radioimmunotherapy utilizing inverse electron demand diels-alder click chemistry," *Molecular Cancer Therapeutics*, vol. 16, no. 1, pp. 124–133, 2017.

[268] J. Funkhouser, "Reinventing pharma: the theranostic revolution," *Current Drug Discovery*, pp. 17–19, 2002.

[269] J. Sorensen, I. Velikyan, A. Wennborg et al., "Measuring HER2-expression in metastatic breast cancer using 68Ga-ABY025 PET/CT," *European Journal of Nuclear Medicine and Molecular Imaging*, vol. 41, pp. S226–S226, 2014.

[270] I. Velikyan, A. Wennborg, J. Feldwisch et al., "GMP compliant preparation of a 68Gallium-labeled Affibody analogue for breast cancer patient examination: first-in-man," *Eur J Nucl Med Mol Imaging*, vol. 41, pp. S228–S229, 2014.

[271] K. Öberg, "Molecular imaging radiotherapy: Theranostics for personalized patient management of neuroendocrine tumors (NETs)," *Theranostics*, vol. 2, no. 5, pp. 448–458, 2012.

[272] I. Velikyan, A. Wennborg, J. Feldwisch, H. Lindman, J. Carlsson, and J. Sorensen, "Good manufacturing practice production of [(68) Ga]Ga-ABY-025 for HER2 specific breast cancer imaging," *American Journal of Nuclear Medicine and Molecular Imaging*, vol. 6, no. 2, pp. 135–153, 2016.

[273] M. Sandström, K. Lindskog, I. Velikyan et al., "Biodistribution and radiation dosimetry of the anti-HER2 Affibody molecule 68Ga-ABY-025 in breast cancer patients," *Journal of Nuclear Medicine*, vol. 57, no. 6, pp. 867–871, 2016.

[274] D. Sandberg, V. Tolmachev, I. Velikyan et al., "Intra-image referencing for simplified assessment of HER2-expression in breast cancer metastases using the Affibody molecule ABY-025 with PET and SPECT," *European Journal of Nuclear Medicine and Molecular Imaging*, vol. 44, no. 8, pp. 1337–1346, 2017.

[275] H. Zhang, M. A. Moroz, I. Serganova et al., "Imaging expression of the human somatostatin receptor subtype-2 reporter gene with 68Ga-DOTATOC," *Journal of Nuclear Medicine*, vol. 52, no. 1, pp. 123–131, 2011.

[276] M. Naji and A. Al-Nahhas, "68Ga-labelled peptides in the management of neuroectodermal tumours," *European Journal of Nuclear Medicine and Molecular Imaging*, vol. 39, no. 1, pp. S61–S67, 2012.

[277] I. Velikyan, "The diversity of 68Ga-Based imaging agents," *Recent Results in Cancer Research*, vol. 194, pp. 101–131, 2013.

[278] K. Ferreira, H-Y. Hu, V. Fetz et al., "Multivalent siderophore-dotam conjugates as theranostics for imaging and treatment of bacterial infections," *Angewandte Chemie International Edition*, vol. 56, no. 28, pp. 8272–8276, 2017.